ORTHOGONAL POLYNOMIAL EXPANSIONS FOR SOLVING RANDOM EIGENVALUE PROBLEMS

*Sharif Rahman** & *Vaibhav Yadav*

College of Engineering and Program of Applied Mathematical and Computational Sciences, The University of Iowa, Iowa City, IA 52242

This paper examines two stochastic methods stemming from polynomial dimensional decomposition (PDD) and polynomial chaos expansion (PCE) for solving random eigenvalue problems commonly encountered in dynamics of mechanical systems. Although the infinite series from PCE and PDD are equivalent, their truncations endow contrasting dimensional structures, creating significant differences between the resulting PDD and PCE approximations in terms of accuracy, efficiency, and convergence properties. When the cooperative effects of input variables on an eigenvalue attenuate rapidly or vanish altogether, the PDD approximation commits a smaller error than does the PCE approximation for identical expansion orders. Numerical analyses of mathematical functions or simple dynamic systems reveal markedly higher convergence rates of the PDD approximation than the PCE approximation. From the comparison of computational efforts, required to estimate with the same precision the frequency distributions of dynamic systems, including a piezoelectric transducer, the PDD approximation is significantly more efficient than the PCE approximation.

KEY WORDS: *stochastic mechanics, random matrix, polynomial dimensional decomposition, polynomial chaos expansion, piezoelectric transducer*

1. INTRODUCTION

Random eigenvalue problems (REPs) comprising stochastic matrix, differential, or integral operators frequently appear in many fields of engineering, science, and mathematics. They are commonly solved by stochastic methods that determine the statistical moments, probability law, and other relevant properties of eigensolutions. The solutions may represent oscillatory modes of a mechanical or structural system (e.g., vehicles, buildings, bridges), disposition of electrons around an atom or a molecule, acoustic modes of a concert hall, eigenfaces in computer vision technology, spectral properties of a graph, and numerous other physical or mathematical quantities.

Many REPs are focused on the second-moment properties of eigensolutions, for which there exist a multitude of methods or approaches. Prominent among them are the classical perturbation method [1], the iteration method [1], the Ritz method [2], the crossing theory [3], the stochastic reduced basis approach [4], and the asymptotic method [5]. More recent developments on solving REPs include the stochastic expansion methods, notably, the polynomial chaos expansion (PCE) [6] and polynomial dimensional decomposition (PDD) [7] methods, both employing Fourier expansions in terms of orthogonal polynomials for approximating eigensolutions. The latter two methods also provide the probability distributions of eigensolutions, although the concomitant approximations are guaranteed to converge only in the mean-square sense, provided that the eigensolutions are square-integrable functions of the random input with respect to its probability measure. A distinguishing feature of these expansion methods is their effective exploitation of the smoothness properties of eigensolutions, if they exist, with the attendant convergence rates markedly higher than those obtained from the sampling-based methods. However, due to the contrasting dimensional structures of PDD and PCE, the convergence properties of their truncations are not the same and may differ significantly, depending on the eigensolution and dimension of the problem. Therefore, uncovering their mathematical properties, which have

---

*Correspond to Sharif Rahman, E-mail: rahman@engineering.uiowa.edu

ramifications in stochastic computing, including solving REPs, is a major motivation for this current work. Is PDD superior to PCE or vice versa? It is also desirable to compare the errors from the PDD and PCE approximations and thereby establish appropriate criteria for grading these two methods.

This paper presents a rigorous comparison of the PDD and PCE methods for calculating the statistical moments and tail probability distributions of random eigenvalues commonly encountered in dynamics of mechanical systems. The methods are based on (i) a broad range of orthonormal polynomial bases consistent with the probability measure of the random input and (ii) an innovative dimension-reduction integration for calculating the expansion coefficients. Section 2 formally defines the REP addressed in this study. Section 3 provides a brief exposition of PDD and PCE, including establishing the relationship between the two expansions. Section 4 discusses PDD and PCE approximations resulting from series truncations, where an alternative form of the PCE approximation has been derived, leading to approximate probabilistic solutions from both methods in terms of the PDD expansion coefficients. Section 4 also presents an error analysis due to PDD and PCE approximations. Section 5 describes the dimension-reduction integration for estimating the PDD expansion coefficients, including the computational efforts required. Five numerical examples illustrate the accuracy, convergence, and computational efficiency of the PDD and PCE methods in Section 6. Finally, conclusions are drawn in Section 7.

2. EIGENVALUE PROBLEMS IN STOCHASTIC DYNAMICS

Let $(\Omega, \mathcal{F}, P)$ be a complete probability space, where Ω is a sample space, $\mathcal{F}$ is a σ-field on Ω, and $P : \mathcal{F} \to [0, 1]$ is a probability measure. Let $\mathbb{R}^N$ and $\mathbb{C}^N$ be N-dimensional real and complex vectors spaces, respectively, and $\mathbb{R}^{N \times N}$ a set of all $N \times N$, real-valued matrices. With $\mathcal{B}^N$ representing a Borel σ-field on $\mathbb{R}^N$ and $\mathbb{E}$ the expectation operator on $(\Omega, \mathcal{F}, P)$, consider an $\mathbb{R}^N$-valued, independent, input random vector $\{\boldsymbol{X} = \{X_1, \ldots, X_N\}^T : (\Omega, \mathcal{F}) \to (\mathbb{R}^N, \mathcal{B}^N)\}$, which has mean vector $\boldsymbol{\mu_X} := \mathbb{E}[\boldsymbol{X}] \in \mathbb{R}^N$, covariance matrix $\boldsymbol{\Sigma_X} := \mathbb{E}[(\boldsymbol{X} - \boldsymbol{\mu_X})(\boldsymbol{X} - \boldsymbol{\mu_X})^T] \in \mathbb{R}^{N \times N}$, and joint probability density function $f_{\boldsymbol{X}}(\boldsymbol{x}) = \Pi_{i=1}^{i=N} f_i(x_i)$, where $f_i(x_i)$ is the marginal probability density function of X_i defined on the probability triple $(\Omega_i, \mathcal{F}_i, P_i)$. In most dynamic systems, the vector $\boldsymbol{X}$ represents uncertainties in material parameters (e.g., mass, damping, stiffness), geometry (e.g., size, shape, topology), and constraints (e.g., initial and boundary conditions).

Consider a family of $L \times L$, real-valued, random coefficient matrices $\boldsymbol{A}_j(\boldsymbol{X}) \in \mathbb{R}^{L \times L}$, $j = 1, \ldots, J$, where J is a positive integer and a general nonlinear function f. The probabilistic characteristics of $\boldsymbol{A}_j(\boldsymbol{X})$ can be derived from the known probability law of $\boldsymbol{X}$. A nontrivial solution of

$$f\left[\lambda(\boldsymbol{X}); \boldsymbol{A}_1(\boldsymbol{X}), \ldots, A_J(\boldsymbol{X})\right] \boldsymbol{\phi}(\boldsymbol{X}) = \boldsymbol{0}, \tag{1}$$

if it exists, defines the random eigenvalue $\lambda(\boldsymbol{X}) \in \mathbb{R}$ or $\mathbb{C}$ and the random eigenvector $\boldsymbol{\phi}(\boldsymbol{X}) \in \mathbb{R}^L$ or $\mathbb{C}^L$ of a general nonlinear eigenvalue problem. Depending on the type of application, a wide variety of functions f and, hence, eigenvalue problems exist. Table 1 shows a few examples of REPs frequently encountered in dynamic systems. In general, the eigensolutions depend on the random input $\boldsymbol{X}$ via solution of the matrix characteristic equation

$$\det\left\{f\left[\lambda(\boldsymbol{X}); \boldsymbol{A}_1(\boldsymbol{X}), \ldots, \boldsymbol{A}_J(\boldsymbol{X})\right]\right\} = 0 \tag{2}$$

and subsequent solution of Eq. (1). A major objective in solving a random eigenvalue problem is to find the probabilistic characteristics of eigenpairs $\{\lambda^{(i)}(\boldsymbol{X}), \boldsymbol{\phi}^{(i)}(\boldsymbol{X})\}$, $i = 1, \ldots, L$, when the probability law of $\boldsymbol{X}$ is arbitrarily prescribed. Both the PDD and PCE methods can be employed to solve any REP in Table 1, however, yielding different accuracy or efficiency with significant implications in stochastic computing. Therefore, a rigorous comparison of these two expansion methods—the principal focus of this work—should provide deeper insights into their respective capabilities as well as limitations.

3. STOCHASTIC EIGENVALUE EXPANSIONS

Let $\lambda(\boldsymbol{X})$, a real-valued, mean-square integrable, measurable transformation on $(\Omega, \mathcal{F})$, define a relevant eigenvalue of a stochastic dynamic system. In general, the multivariate function $\lambda : \mathbb{R}^N \to \mathbb{R}$ is implicit, is not analytically

TABLE 1: Random eigenvalue problems in stochastic dynamical systems

Eigenvalue problem[a]	Problem type and application(s)
$[-\lambda(\boldsymbol{X})\boldsymbol{M}(\boldsymbol{X}) + \boldsymbol{K}(\boldsymbol{X})]\,\boldsymbol{\phi}(\boldsymbol{X}) = \boldsymbol{0}$	*Linear:* undamped or proportionally damped systems
$[\lambda^2(\boldsymbol{X})\boldsymbol{M}(\boldsymbol{X}) + \lambda(\boldsymbol{X})\boldsymbol{C}(\boldsymbol{X}) + \boldsymbol{K}(\boldsymbol{X})]\,\boldsymbol{\phi}(\boldsymbol{X}) = \boldsymbol{0}$	*Quadratic:* non-proportionally damped systems, singularity problems
$[\lambda(\boldsymbol{X})\boldsymbol{M}_1(\boldsymbol{X}) + \boldsymbol{M}_0(\boldsymbol{X}) + \boldsymbol{M}_1^T(\boldsymbol{X})/\lambda(\boldsymbol{X})]\,\boldsymbol{\phi}(\boldsymbol{X}) = \boldsymbol{0}$	*Palindromic:* acoustic emissions in high-speed trains
$\left[\sum_k \lambda^k(\boldsymbol{X})\boldsymbol{A}_k(\boldsymbol{X})\right]\boldsymbol{\phi}(\boldsymbol{X}) = \boldsymbol{0}$	*Polynomial:* control and dynamics problems
$\left[\lambda(\boldsymbol{X})\boldsymbol{M}(\boldsymbol{X}) - \boldsymbol{K}(\boldsymbol{X}) + \sum_k \dfrac{\lambda^q(\boldsymbol{X})\boldsymbol{C}_k(\boldsymbol{X})}{a_k - \lambda(\boldsymbol{X})}\right]\boldsymbol{\phi}(\boldsymbol{X}) = \boldsymbol{0}$	*Rational:* plate vibration ($q = 1$), fluid-structure vibration ($q = 2$), vibration of viscoelastic materials

[a] $\boldsymbol{M}(\boldsymbol{X})$, $\boldsymbol{C}(\boldsymbol{X})$, and $\boldsymbol{K}(\boldsymbol{X})$ are mass, damping, stiffness matrices, respectively; $\boldsymbol{M}_0(\boldsymbol{X})$, $\boldsymbol{M}_1(\boldsymbol{X})$, $\boldsymbol{A}_k(\boldsymbol{X})$, and $\boldsymbol{C}_k(\boldsymbol{X})$ are various coefficient matrices.

available, and can only be viewed as a high-dimensional input-output mapping, where the evaluation of the output function λ for a given input $\boldsymbol{X}$ requires expensive finite element analysis (FEA). Therefore, methods employed in stochastic analysis must be capable of generating accurate probabilistic characteristics of $\lambda(\boldsymbol{X})$ with an acceptably small number of output function evaluations.

3.1 Orthonormal Polynomials

Let $\mathcal{L}_2(\Omega_i, \mathcal{F}_i, P_i)$ be a Hilbert space that is equipped with a set of complete orthonormal bases $\{\psi_{ij}(x_i); j = 0, 1, \ldots\}$, which is consistent with the probability measure of X_i. For example, classical orthonormal polynomials, including Hermite, Legendre, and Jacobi polynomials, can be used when X_i follows Gaussian, uniform, and β probability distributions, respectively [8]. For an arbitrary measure, approximate methods based on the Stieltjes procedure can be employed to obtain the associated orthonormal polynomials [8, 9]. If $\mathbb{E}$ is the expectation operator with respect to the probability measure of $\boldsymbol{X}$, then two important properties of orthonormal polynomials are as follows [9, 10].

Property 1. *The orthonormal polynomial basis functions have a unit mean for $j = 0$ and zero means for all $j \geq 1$, i.e.,*

$$\mathbb{E}[\psi_{ij}(X_i)] := \int_{\mathbb{R}} \psi_{ij}(x_i)f_i(x_i)dx_i = \begin{cases} 1 & \text{if } j = 0, \\ 0 & \text{if } j \geq 1. \end{cases} \tag{3}$$

Property 2. *Any two orthonormal polynomial basis functions $\psi_{ij_1}(X_i)$ and $\psi_{ij_2}(X_i)$, where $j_1, j_2 = 0, 1, 2, \ldots$, are uncorrelated and each has unit variance, i.e.,*

$$\mathbb{E}[\psi_{ij_1}(X_i)\psi_{ij_2}(X_i)] := \int_{\mathbb{R}} \psi_{ij_1}(x_i)\psi_{ij_2}(x_i)f_i(x_i)dx_i = \begin{cases} 1 & \text{if } j_1 = j_2, \\ 0 & \text{if } j_1 \neq j_2. \end{cases} \tag{4}$$

If λ is a sufficiently smooth function of $\boldsymbol{X}$, then there exist two important stochastic expansions of random eigenvalues involving orthonormal polynomials, as follows.

3.2 Polynomial dimensional decomposition

The PDD of a random eigenvalue $\lambda(\boldsymbol{X})$ represents a finite, hierarchical expansion [7, 9]

$$
\begin{aligned}
\lambda_{\mathrm{PDD}}(\boldsymbol{X}) \quad := \quad & \lambda_0 + \sum_{i=1}^{N}\sum_{j=1}^{\infty} C_{ij}\psi_{ij}(X_i) + \sum_{i_1=1}^{N-1}\sum_{i_2=i_1+1}^{N}\sum_{j_2=1}^{\infty}\sum_{j_1=1}^{\infty} C_{i_1 i_2 j_1 j_2}\psi_{i_1 j_1}(X_{i_1})\psi_{i_2 j_2}(X_{i_2}) \\
+ \quad & \sum_{i_1=1}^{N-2}\sum_{i_2=i_1+1}^{N-1}\sum_{i_3=i_2+1}^{N}\sum_{j_3=1}^{\infty}\sum_{j_2=1}^{\infty}\sum_{j_1=1}^{\infty} C_{i_1 i_2 i_3 j_1 j_2 j_3}\psi_{i_1 j_1}(X_{i_1})\psi_{i_2 j_2}(X_{i_2})\psi_{i_3 j_3}(X_{i_3}) \\
+ \quad & \dots + \sum_{i_1=1}^{1}\cdots\sum_{i_N=i_{N-1}+1}^{N}\sum_{j_N=1}^{\infty}\cdots\sum_{j_1=1}^{\infty} C_{i_1\dots i_N j_1\dots j_N}\prod_{q=1}^{N}\psi_{i_q j_q}(X_{i_q}) \\
= \quad & \lambda_0 + \sum_{s=1}^{N}\left[\underbrace{\sum_{i_1=1}^{N-s+1}\cdots\sum_{i_s=i_{s-1}+1}^{N}}_{s\ \text{sums}}\ \underbrace{\sum_{j_1=1}^{\infty}\cdots\sum_{j_s=1}^{\infty}}_{s\ \text{sums}} C_{i_1\dots i_s j_1\dots j_s}\prod_{q=1}^{s}\psi_{i_q j_q}(X_{i_q})\right]
\end{aligned}
\tag{5}
$$

in terms of random orthonormal polynomials $\psi_{ij}(X_i)$, $i = 1,\dots,N$; $j = 1,\dots,\infty$ of input variables $X_1,\dots,X_N$ with increasing dimensions, where

$$
\lambda_0 := \int_{\mathbb{R}^N} \lambda(\boldsymbol{x}) f_{\boldsymbol{X}}(\boldsymbol{x}) d\boldsymbol{x}
\tag{6}
$$

and

$$
C_{i_1\dots i_s j_1\dots j_s} := \int_{\mathbb{R}^N} \lambda(\boldsymbol{x}) \prod_{q=1}^{s} \psi_{i_q j_q}(x_{i_q}) f_{\boldsymbol{X}}(\boldsymbol{x}) d\boldsymbol{x},
\tag{7}
$$

for $s = 1,\dots,N$, $1 \le i_1 < \dots < i_s \le N$, $j_1,\dots,j_s = 1,\dots,\infty$ are the associated expansion coefficients, which require calculating various high-dimensional integrals when N is large. In Eq. (5), the term $\sum_{j_s=1}^{\infty}\cdots\sum_{j_1=1}^{\infty}C_{i_1\dots i_s j_1\dots j_s}\prod_{q=1}^{s}\psi_{i_q j_q}(X_{i_q})$ represents the s-variate component function, quantifying the cooperative effect of s input variables $X_{i_1},\dots,X_{i_S}$ on λ.

3.3 Polynomial Chaos Expansion

The PCE of a random eigenvalue $\lambda(\boldsymbol{X})$, a function of a finite number of random variables $X_1,\dots,X_N$, has a representation [11–13]

$$
\begin{aligned}
\lambda_{\mathrm{PCE}}(\boldsymbol{X}) := \ & a_0\Gamma_0 + \sum_{i=1}^{N} a_i\Gamma_1(X_i) + \sum_{i_1=1}^{N}\sum_{i_2=i_1}^{N} a_{i_1 i_2}\Gamma_2(X_{i_1}, X_{i_2}) + \sum_{i_1=1}^{N}\sum_{i_2=i_1}^{N}\sum_{i_3=i_2}^{N} a_{i_1 i_2 i_3}\Gamma_3(X_{i_1}, X_{i_2}, X_{i_3}) \\
& + \ \dots + \sum_{i_1=1}^{N}\cdots\sum_{i_p=i_{p-1}}^{N} a_{i_1\dots i_p}\Gamma_p(X_{i_1},\dots,X_{i_p}) + \dots
\end{aligned}
\tag{8}
$$

in terms of random polynomial chaoses, $\Gamma_p(X_{i_1},\dots,X_{i_p})$, $p = 0,\dots,\infty$, $1 \le i_1 \le \dots \le i_p \le N$, of input variables $X_{i_1},\dots,X_{i_p}$ with increasing orders, where

$$
a_0 := \int_{\mathbb{R}^N} \lambda(\boldsymbol{x})\Gamma_0 f_{\boldsymbol{X}}(\boldsymbol{x}) d\boldsymbol{x}
\tag{9}
$$

and

$$
a_{i_1\dots i_p} := \int_{\mathbb{R}^N} \lambda(\boldsymbol{x})\Gamma_p(X_{i_1},\dots,X_{i_p}) f_{\boldsymbol{X}}(\boldsymbol{x}) d\boldsymbol{x},
\tag{10}
$$

for $p = 1,\dots,\infty$, $1 \le i_1 \le \dots \le i_p \le N$, are the corresponding expansion coefficients that also require evaluating high-dimensional integrals.

Once the expansion coefficients in Eq. (5) or (8) are determined, as explained in a forthcoming section, PDD and PCE furnish surrogates of the exact map $\lambda : \mathbb{R}^N \to \mathbb{R}$, describing an input-output relationship from a complicated numerical eigenvalue analysis. Therefore, any probabilistic characteristic of $\lambda(\boldsymbol{X})$, including its statistical moments and rare event probabilities, can be estimated from its PDD or PCE.

Remark 1. Using Properties 1 and 2 of orthonormal polynomials, it is elementary to show that the second-moment properties of any mean-square integrable function $\lambda(\boldsymbol{X})$, its PDD $\lambda_{\mathrm{PDD}}(\boldsymbol{X})$, and its PCE $\lambda_{\mathrm{PCE}}(\boldsymbol{X})$ are identical. In other words, $\lambda(\boldsymbol{X})$, $\lambda_{\mathrm{PDD}}(\boldsymbol{X})$, and $\lambda_{\mathrm{PCE}}(\boldsymbol{X})$ are equivalent in the mean-square sense.

3.4 Relationship between PDD and PCE

Because the polynomial chaoses in Eq. (8) are built from univariate orthonormal polynomials, PDD and PCE are related. Indeed, there exists a striking theorem, as follows.

Theorem 1. *If $\lambda_{\mathrm{PDD}}(\boldsymbol{X})$ and $\lambda_{\mathrm{PCE}}(\boldsymbol{X})$ are two infinite series defined in Eqs. (5) and (8), respectively, then one series can be rearranged to derive the other series, for instance, $\lambda_{\mathrm{PCE}}(\boldsymbol{X}) = \lambda_{\mathrm{PDD}}(\boldsymbol{X})$.*

Proof. The polynomial chaoses $\Gamma_p(X_{i_1}, \ldots, X_{i_p})$, $p = 0, \ldots, \infty$, $1 \le i_1 \le \ldots \le i_p \le N$ in Eq. (8) can be more explicitly written as

$$
\begin{aligned}
\Gamma_0 &= 1 \\
\Gamma_1(X_i) &= \psi_{i1}(X_i) \\
\Gamma_2(X_{i_1}, X_{i_2}) &= \psi_{i_2 2}(X_{i_1})\delta_{i_1 i_2} - \psi_{i_1 1}(X_{i_1})\psi_{i_2 1}(X_{i_2})(\delta_{i_1 i_2} - 1) \\
\Gamma_3(X_{i_1}, X_{i_2}, X_{i_3}) &= \psi_{i_3 3}(X_{i_1})\delta_{i_1 i_2}\delta_{i_1 i_3}\delta_{i_2 i_3} \\
&\quad - \psi_{i_1 1}(X_{i_1})\psi_{i_2 2}(X_{i_2})\delta_{i_2 i_3}(\delta_{i_1 i_2} - 1) \\
&\quad - \psi_{i_2 2}(X_{i_2})\psi_{i_3 1}(X_{i_3})\delta_{i_1 i_2}(\delta_{i_2 i_3} - 1) \\
&\quad - \psi_{i_1 1}(X_{i_1})\psi_{i_2 1}(X_{i_2})\psi_{i_3 1}(X_{i_3})(\delta_{i_1 i_2}\delta_{i_1 i_3}\delta_{i_2 i_3} - 1)(\delta_{i_1 i_2} - 1)(\delta_{i_2 i_3} - 1) \\
\ldots &= \ldots,
\end{aligned}
\tag{11}
$$

which represents various combinations of tensor products of sets of univariate orthonormal polynomials with $\delta_{i_k i_l}$, $k, l = 1, \ldots, p$, denoting various Kronecker deltas, i.e., $\delta_{i_k i_l} = 1$ when $i_k = i_l$ and zero otherwise. Inserting Eq. (11) into Eqs. (9) and (10) with Eqs. (6) and (7) in mind, the PCE coefficients,

$$
\begin{aligned}
a_0 &= \lambda_0 \\
a_i &= C_{i1} \\
a_{i_1 i_2} &= C_{i_1 2}\delta_{i_1 i_2} - C_{i_1 i_2 11}(\delta_{i_1 i_2} - 1) \\
a_{i_1 i_2 i_3} &= C_{i_1 3}\delta_{i_1 i_2}\delta_{i_1 i_3}\delta_{i_2 i_3} - C_{i_1 i_2 12}\delta_{i_2 i_3}(\delta_{i_1 i_2} - 1) \\
&\quad - C_{i_2 i_3 21}\delta_{i_1 i_2}(\delta_{i_2 i_3} - 1) \\
&\quad - C_{i_1 i_2 i_3 111}(\delta_{i_1 i_2}\delta_{i_1 i_3}\delta_{i_2 i_3} - 1)(\delta_{i_1 i_2} - 1)(\delta_{i_2 i_3} - 1) \\
\ldots &= \ldots,
\end{aligned}
\tag{12}
$$

provide explicit connections to the PDD coefficients. Using the polynomial chaoses and PCE coefficients from Eqs. (11) and (12), respectively, and after some simplifications, the zero- to higher-order PCE terms become

$$a_0 \Gamma_0 = \lambda_0$$

$$\sum_{i=1}^{N} a_i \Gamma_1(X_i) = \sum_{i=1}^{N} C_{i1}\psi_{i1}(X_i)$$

$$\sum_{i_1=1}^{N}\sum_{i_2=i_1}^{N} a_{i_1 i_2}\Gamma_2(X_{i_1}, X_{i_2}) = \sum_{i=1}^{N} C_{i2}\psi_{i2}(X_i) + \sum_{i_1,i_2=1;i_1<i_2}^{N} C_{i_1 i_2 11}\psi_{i_1 1}(X_{i_1})\psi_{i_2 1}(X_{i_2})$$

$$\sum_{i_1=1}^{N}\sum_{i_2=i_1}^{N}\sum_{i_3=i_2}^{N} a_{i_1 i_2 i_3}\Gamma_3(X_{i_1}, X_{i_2}, X_{i_3}) = \sum_{i=1}^{N} C_{i3}\psi_{i3}(X_i) + \sum_{i_1,i_2=1;i_1<i_2}^{N} C_{i_1 i_2 12}\psi_{i_1 1}(X_{i_1})\psi_{i_2 2}(X_{i_2}) \qquad (13)$$

$$+ \sum_{i_1,i_2=1;i_1<i_2}^{N} C_{i_2 i_3 21}\psi_{i_1 2}(X_{i_1})\psi_{i_2 1}(X_{i_2})$$

$$+ \sum_{i_1,i_2,i_3=1;i_1<i_2<i_3}^{N} C_{i_1 i_2 i_3 111}\psi_{i_1 1}(X_{i_1})\psi_{i_2 1}(X_{i_2})\psi_{i_3 1}(X_{i_3})$$

$$\ldots = \ldots,$$

revealing constituents comprising constant, univariate functions, bivariate functions, etc. Collecting all univariate terms, all bivariate terms, etc., from each appropriate line of Eq. (13) leads to

$$\lambda_{\mathrm{PCE}}(\boldsymbol{X}) = \lim_{p\to\infty}\left[\lambda_0 + \sum_{i=1}^{N}\sum_{j=1}^{p} C_{ij}\psi_{ij}(X_i) + \sum_{i_1=1}^{N-1}\sum_{i_2=i_1+1}^{N}\underbrace{\sum_{j_2=1}^{p-1}\sum_{j_1=1}^{p-1}}_{j_1+j_2\leq p} C_{i_1 i_2 j_1 j_2}\psi_{i_1 j_1}(X_{i_1})\psi_{i_2 j_2}(X_{i_2})\right.$$

$$+ \sum_{i_1=1}^{N-2}\sum_{i_2=i_1+1}^{N-1}\sum_{i_3=i_2+1}^{N}\underbrace{\sum_{j_3=1}^{p-2}\sum_{j_2=1}^{p-2}\sum_{j_1=1}^{p-2}}_{j_1+j_2+j_3\leq p} C_{i_1 i_2 i_3 j_1 j_2 j_3}\psi_{i_1 j_1}(X_{i_1})\psi_{i_2 j_2}(X_{i_2})\psi_{i_3 j_3}(X_{i_3})$$

$$\left.+ \ldots + \sum_{i_1=1}^{1}\cdots\sum_{i_N=i_{N-1}+1}^{N}\underbrace{\sum_{j_N=1}^{p-N+1}\cdots\sum_{j_1=1}^{p-N+1}}_{j_1+\ldots+j_N\leq p} C_{i_1\ldots i_N j_1\ldots j_N}\prod_{q=1}^{N}\psi_{i_q j_q}(X_{i_q})\right]$$

$$= \lambda_0 + \sum_{i=1}^{N}\sum_{j=1}^{\infty} C_{ij}\psi_{ij}(X_i) + \sum_{i_1=1}^{N-1}\sum_{i_2=i_1+1}^{N}\sum_{j_2=1}^{\infty}\sum_{j_1=1}^{\infty} C_{i_1 i_2 j_1 j_2}\psi_{i_1 j_1}(X_{i_1})\psi_{i_2 j_2}(X_{i_2})$$

$$+ \sum_{i_1=1}^{N-2}\sum_{i_2=i_1+1}^{N-1}\sum_{i_3=i_2+1}^{N}\sum_{j_3=1}^{\infty}\sum_{j_2=1}^{\infty}\sum_{j_1=1}^{\infty} C_{i_1 i_2 i_3 j_1 j_2 j_3}\psi_{i_1 j_1}(X_{i_1})\psi_{i_2 j_2}(X_{i_2})\psi_{i_3 j_3}(X_{i_3})$$

$$+ \ldots + \sum_{i_1=1}^{1}\cdots\sum_{i_N=i_{N-1}+1}^{N}\sum_{j_N=1}^{\infty}\cdots\sum_{j_1=1}^{\infty} C_{i_1\ldots i_N j_1\ldots j_N}\prod_{q=1}^{N}\psi_{i_q j_q}(X_{i_q})$$

$$= \lambda_0 + \sum_{s=1}^{N}\left[\underbrace{\sum_{i_1=1}^{N-s+1}\cdots\sum_{i_s=i_{s-1}+1}^{N}}_{s\ \text{sums}}\ \underbrace{\sum_{j_1=1}^{\infty}\cdots\sum_{j_s=1}^{\infty}}_{s\ \text{sums}} C_{i_1\ldots i_s j_1\ldots j_s}\prod_{q=1}^{s}\psi_{i_q j_q}(X_{i_q})\right] =: \lambda_{\mathrm{PDD}}(\boldsymbol{X}),$$

$$(14)$$

which proves the theorem for any mean-square integrable function $\lambda : \mathbb{R}^N \to \mathbb{R}$, $1 \leq N < \infty$, and probability distribution of $\boldsymbol{X}$.

4. SERIES TRUNCATIONS AND APPROXIMATE SOLUTIONS

4.1 PDD Approximation

Although Eq. (5) provides an exact PDD representation, it contains an infinite number of coefficients, emanating from infinite numbers of orthonormal polynomials. In practice, the number of coefficients must be finite, say, by retaining at most mth-order polynomials in each variable. Furthermore, in many applications, the function λ can be approximated by a sum of at most S-variate component functions, where $1 \le S \le N$ is another truncation parameter, resulting in the S-variate, mth-order PDD approximation

$$\tilde{\lambda}_{S,m}(\boldsymbol{X}) = \lambda_0 + \sum_{s=1}^{S}\left[\underbrace{\sum_{i_1=1}^{N-s+1}\cdots\sum_{i_s=i_{s-1}+1}^{N}}_{s \text{ sums}} \underbrace{\sum_{j_1=1}^{m}\cdots\sum_{j_s=1}^{m}}_{s \text{ sums}} C_{i_1\ldots i_s j_1\ldots j_s} \prod_{q=1}^{s}\psi_{i_q j_q}(X_{i_q})\right], \tag{15}$$

containing

$$Q_{S,m} = \sum_{k=0}^{S}\binom{N}{S-k}m^{S-k} \tag{16}$$

number of PDD coefficients and corresponding orthonormal polynomials. The PDD approximation in Eq. (15) includes cooperative effects of at most S input variables $X_{i_1}, \ldots, X_{i_S}, 1 \le i_1 \le \ldots \le i_S \le N$, on λ. For instance, by selecting $S = 1$ and 2, the functions, $\tilde{\lambda}_{1,m}(\boldsymbol{X})$ and $\tilde{\lambda}_{2,m}(\boldsymbol{X})$, respectively, provide univariate and bivariate mth-order approximations, contain contributions from all input variables, and should not be viewed as first- and second-order approximations, nor do they limit the nonlinearity of $\lambda(\boldsymbol{X})$. Depending on how the component functions are constructed, arbitrarily high-order univariate and bivariate terms of $\lambda(\boldsymbol{X})$ could be lurking inside $\tilde{\lambda}_{1,m}(\boldsymbol{X})$ and $\tilde{\lambda}_{2,m}(\boldsymbol{X})$. The fundamental conjecture underlying this decomposition is that the component functions arising in the function decomposition will exhibit insignificant S-variate effects cooperatively when $S \to N$, leading to useful lower-variate approximations of $\lambda(\boldsymbol{X})$. When $S \to N$ and $m \to \infty$, $\tilde{\lambda}_{S,m}(\boldsymbol{X})$ converges to $\lambda(\boldsymbol{X})$ in the mean-square sense, i.e., Eq. (15) generates a hierarchical and convergent sequence of approximations of $\lambda(\boldsymbol{X})$.

Applying the expectation operator on Eq. (15) and noting property 1, the mean $\mathbb{E}\left[\tilde{\lambda}_{S,m}(\boldsymbol{X})\right] = \lambda_0$ of the S-variate, mth-order approximation of the eigenvalue matches the exact mean of the eigenvalue in Eq. (6), regardless of S or m. Applying the expectation operator again, this time on $\left[\tilde{\lambda}_{S,m}(\boldsymbol{X}) - \lambda_0\right]^2$, results in the approximate variance

$$\mathbb{E}\left[\tilde{\lambda}_{S,m}(\boldsymbol{X}) - \lambda_0\right]^2 = \sum_{s=1}^{S}\sum_{t=1}^{S}\left(\underbrace{\sum_{i_1=1}^{N-s+1}\cdots\sum_{i_s=i_{s-1}+1}^{N}\sum_{j_1=1}^{m}\cdots\sum_{j_s=1}^{m}}_{2s \text{ sums}}\underbrace{\sum_{k_1=1}^{N-t+1}\cdots\sum_{k_t=k_{t-1}+1}^{N}\sum_{l_1=1}^{m}\cdots\sum_{l_t=1}^{m}}_{2t \text{ sums}}C_{i_1\ldots i_s j_1\ldots j_s}\right.$$
$$\left.\times\; C_{k_1\ldots k_t l_1\ldots l_t}\mathbb{E}\left[\prod_{q=1}^{s}\psi_{i_q j_q}(X_{i_q})\prod_{q=1}^{t}\psi_{k_q l_q}(X_{k_q})\right]\right) \tag{17}$$

of the eigenvalue, which depends on S and m. The number of summations inside the parenthesis of the right side of Eq. (17) is $2(s+t)$, where s and t are the indices of the two outer summations. By virtue of property 2 and independent coordinates of $\boldsymbol{X}$,

$$\mathbb{E}\left[\prod_{q=1}^{s}\psi_{i_q j_q}(X_{i_q})\prod_{q=1}^{t}\psi_{k_q l_q}(X_{k_q})\right] = \prod_{q=1}^{s}\mathbb{E}\left[\psi_{i_q j_q}^2(X_{i_q})\right] = 1 \tag{18}$$

for $s = t$, $i_q = k_q$, $j_q = l_q$ and zero otherwise, leading to

$$\mathbb{E}\left[\tilde{\lambda}_{S,m}(\boldsymbol{X}) - \lambda_0\right]^2 = \sum_{s=1}^{S}\left(\underbrace{\sum_{i_1=1}^{N-s+1}\cdots\sum_{i_s=i_{s-1}+1}^{N}}_{s\text{ sums}}\underbrace{\sum_{j_1=1}^{m}\cdots\sum_{j_s=1}^{m}}_{s\text{ sums}}C_{i_1\ldots i_s j_1\ldots j_s}^2\right) \tag{19}$$

as the sum of squares of the expansion coefficients from the S-variate, mth-order PDD approximation of $\lambda(\boldsymbol{X})$. Clearly, the approximate variance in Eq. (19) approaches the exact variance

$$\mathbb{E}\left[\lambda(\boldsymbol{X}) - \lambda_0\right]^2 = \mathbb{E}\left[\lambda_{\mathrm{PDD}}(\boldsymbol{X}) - \lambda_0\right]^2 = \sum_{s=1}^{N}\left(\underbrace{\sum_{i_1=1}^{N-(s+1)}\cdots\sum_{i_s=i_{s-1}+1}^{N}}_{s\text{ sums}}\underbrace{\sum_{j_1=1}^{\infty}\cdots\sum_{j_s=1}^{\infty}}_{s\text{ sums}}C_{i_1\ldots i_s j_1\ldots j_s}^2\right) \tag{20}$$

of the eigenvalue when $S \to N$ and $m \to \infty$. The mean-square convergence of $\tilde{\lambda}_{S,m}$ is guaranteed as λ and its component functions are all members of the associated Hilbert spaces.

Remark 2. The expansion order m, which is a positive integer, should be interpreted as the largest exponent of a single variable from the monomials (terms) of the PDD approximation. On the basis of the traditional definition, the total order of the multivariate polynomial in the right side of Eq. (15) is Sm, although all monomials with total degree equal to or less than Sm are not present.

4.2 PCE Approximation

The pth-order PCE approximation

$$\begin{aligned}
\bar{\lambda}_p(\boldsymbol{X}) := \ &a_0\Gamma_0 + \sum_{i=1}^{N}a_i\Gamma_1(X_i) + \sum_{i_1=1}^{N}\sum_{i_2=i_1}^{N}a_{i_1 i_2}\Gamma_2(X_{i_1}, X_{i_2}) + \sum_{i_1=1}^{N}\sum_{i_2=i_1}^{N}\sum_{i_3=i_2}^{N}a_{i_1 i_2 i_3}\Gamma_3(X_{i_1}, X_{i_2}, X_{i_3}) \\
&+ \ldots + \sum_{i_1=1}^{N}\cdots\sum_{i_p=i_{p-1}}^{N}a_{i_1\ldots i_p}\Gamma_p(X_{i_1}, \ldots, X_{i_p}),
\end{aligned} \tag{21}$$

obtained directly by truncating the right side of Eq. (8), requires $(N+p)!/(N!p!)$ number of the PCE coefficients. However, since PDD and PCE are related, the terms of Eq. (21) can be rearranged following similar derivations in proving Theorem 1, resulting in

$$\begin{aligned}
\bar{\lambda}_p(\boldsymbol{X}) = \ &\lambda_0 + \sum_{i=1}^{N}\sum_{j=1}^{p}C_{ij}\psi_{ij}(X_i) + \sum_{i_1=1}^{N-1}\sum_{i_2=i_1+1}^{N}\underbrace{\sum_{j_2=1}^{p-1}\sum_{j_1=1}^{p-1}}_{j_1+j_2\leq p}C_{i_1 i_2 j_1 j_2}\psi_{i_1 j_1}(X_{i_1})\psi_{i_2 j_2}(X_{i_2}) \\
&+ \sum_{i_1=1}^{N-2}\sum_{i_2=i_1+1}^{N-1}\sum_{i_3=i_2+1}^{N}\underbrace{\sum_{j_3=1}^{p-2}\sum_{j_2=1}^{p-2}\sum_{j_1=1}^{p-2}}_{j_1+j_2+j_3\leq p}C_{i_1 i_2 i_3 j_1 j_2 j_3}\psi_{i_1 j_1}(X_{i_1})\psi_{i_2 j_2}(X_{i_2})\psi_{i_3 j_3}(X_{i_3}) \\
&+ \ldots + \underbrace{\sum_{i_1=1}^{N-s+1}\cdots\sum_{i_s=i_{s-1}+1}^{N}}\underbrace{\sum_{j_N=1}^{p-N+1}\cdots\sum_{j_1=1}^{p-N+1}}_{j_1+\ldots+j_N\leq p}C_{i_1\ldots i_N j_1\ldots j_N}\prod_{q=1}^{N}\psi_{i_q j_q}(X_{i_q})
\end{aligned} \tag{22}$$

with the generic $(s+1)$th term, $s = 1, \ldots, p$, shown or its abbreviated form

$$\bar{\lambda}_p(\boldsymbol{X}) = \lambda_0 + \sum_{s=1}^{p}\left[\underbrace{\sum_{i_1=1}^{N-s+1}\cdots\sum_{i_s=i_{s-1}+1}^{N}}_{s\text{ sums}}\underbrace{\sum_{j_1=1}^{p-s+1}\cdots\sum_{j_s=1}^{p-s+1}}_{s\text{ sums};\,j_1+\ldots+j_s\leq p}C_{i_1\ldots i_s j_1\ldots j_s}\prod_{q=1}^{s}\psi_{i_q j_q}(X_{i_q})\right], \tag{23}$$

involving solely

$$Q_p = \sum_{k=0}^{N} \binom{N}{N-k} \binom{p}{N-k} \tag{24}$$

number of PDD coefficients and corresponding orthonormal polynomials, where $\binom{p}{N-k}$ should be interpreted as zero when $p < N - k$. It is elementary to show that Q_p matches $(N+p)!/(N!p!)$, the original number of PCE coefficients from Eq. (21). The advantage of Eq. (23) over Eq. (21) is that the PDD coefficients, once determined, can be reused for the PCE approximation, thereby sidestepping calculations of the PCE coefficients.

Applying the expectation operator on Eq. (23) and noting Property 1, the mean $\mathbb{E}\left[\bar{\lambda}_p(\boldsymbol{X})\right] = \lambda_0$ of the pth-order PCE approximation of the eigenvalue also matches the exact mean of the eigenvalue for any expansion order. Applying the expectation operator on $\left[\bar{\lambda}_p(\boldsymbol{X}) - \lambda_0\right]^2$ and following similar arguments as before, the variance of the pth-order PCE approximation of the eigenvalue is

$$\mathbb{E}\left[\bar{\lambda}_p(\boldsymbol{X}) - \lambda_0\right]^2 = \sum_{s=1}^{N} \left(\underbrace{\sum_{i_1=1}^{N-s+1} \cdots \sum_{i_s=i_{s-1}+1}^{N}}_{s \text{ sums}} \underbrace{\sum_{j_1=1}^{p-s+1} \cdots \sum_{j_s=1}^{p-s+1}}_{s \text{ sums}; j_1+\ldots+j_s \leq p} C_{i_1\ldots i_s j_1\ldots j_s}^2 \right), \tag{25}$$

another sum of squares of the PDD expansion coefficients such that $j_1 + \ldots + j_s \leq p$, which also converges to $\mathbb{E}\left[\lambda(\boldsymbol{X}) - \lambda_0\right]^2$ as $p \to \infty$.

Remark 3. Two important observations can be made when comparing the PDD and PCE approximations expressed by Eqs. (15) and (21), respectively. First, the terms in the PCE approximation are organized with respect to the order of polynomials. In contrast, the PDD approximation is structured with respect to the degree of cooperativity between a finite number of random variables. Therefore, significant differences may exist regarding the accuracy, efficiency, and convergence properties of their truncated sum or series. Second, if an eigenvalue response is highly nonlinear but contains rapidly diminishing cooperative effects of multiple random variables, the PDD approximation is expected to be more effective than the PCE approximation. This is because the lower-variate (univariate, bivariate, etc.) terms of the PDD approximation can be just as nonlinear by selecting appropriate values of m in Eq. (15). In contrast, many more terms and expansion coefficients are required to be included in the PCE approximation to capture such high nonlinearity.

Remark 4. Depending on the problem size (N) and truncation parameters (S, m, p), there exist a few special cases where the PDD and PCE approximations coincide: (i) when $N = 1$, the univariate, mth-order PDD and mth-order PCE approximations are the same, i.e., $\tilde{\lambda}_{1,m}(X) = \bar{\lambda}_m(X)$ for any $1 \leq m < \infty$; (ii) for any arbitrary value of N, the univariate, first-order PDD and first-order PCE approximations are the same, i.e., $\tilde{\lambda}_{1,1}(\boldsymbol{X}) = \bar{\lambda}_1(\boldsymbol{X})$.

Remark 5. The PDD and PCE approximations, regardless of the truncation parameters, predict the exact mean of an eigenvalue. However, the calculated variances of an eigenvalue from Eqs. (19) and (25) for $S < N$, $m < \infty$, and $p < \infty$ are neither the same nor exact, in general. Therefore, an error analysis, at least pertaining to the second-moment properties of eigensolutions, is required for comparing the PDD and PCE approximations.

4.3 Error Analysis

Define two errors,

$$\begin{aligned} e_{S,m} &:= \mathbb{E}\left[\lambda(\boldsymbol{X}) - \tilde{\lambda}_{S,m}(\boldsymbol{X})\right]^2 = \mathbb{E}\left[\lambda_{\text{PDD}}(\boldsymbol{X}) - \tilde{\lambda}_{S,m}(\boldsymbol{X})\right]^2 \\ &= \int_{\mathbb{R}^N} \left[\lambda_{\text{PDD}}(\boldsymbol{x}) - \tilde{\lambda}_{S,m}(\boldsymbol{x})\right]^2 f_{\boldsymbol{X}}(\boldsymbol{x}) d\boldsymbol{x} \end{aligned} \tag{26}$$

and

$$\begin{aligned} e_p &:= \mathbb{E}\left[\lambda(\boldsymbol{X}) - \bar{\lambda}_p(\boldsymbol{X})\right]^2 = \mathbb{E}\left[\lambda_{\text{PDD}}(\boldsymbol{X}) - \bar{\lambda}_p(\boldsymbol{X})\right]^2 \\ &= \int_{\mathbb{R}^N} \left[\lambda_{\text{PDD}}(\boldsymbol{x}) - \bar{\lambda}_p(\boldsymbol{x})\right]^2 f_{\boldsymbol{X}}(\boldsymbol{x}) d\boldsymbol{x}, \end{aligned} \tag{27}$$

owing to S-variate, mth-order PDD approximation $\tilde{\lambda}_{S,m}(\boldsymbol{X})$ and pth-order PCE approximation $\bar{\lambda}_p(\boldsymbol{X})$, respectively, of $\lambda(\boldsymbol{X})$. Replacing λ_{PDD}, $\tilde{\lambda}_{S,m}$, and $\bar{\lambda}_p$ in Eqs. (26) and (27) with the right sides of Eqs. (5), (15), and (23), respectively, and invoking properties 1 and 2 yields the PDD error

$$
\begin{aligned}
e_{S,m} = \sum_{s=1}^{S}\Bigg(&\underbrace{\sum_{i_1=1}^{N-s+1}\cdots\sum_{i_s=i_{s-1}+1}^{N}}_{s\ \text{sums}}\ \underbrace{\sum_{j_1=m+1}^{\infty}\cdots\sum_{j_s=m+1}^{\infty}}_{s\ \text{sums}} C_{i_1\ldots i_s j_1\ldots j_s}^2 \Bigg) \\
+ \sum_{s=S+1}^{N}\Bigg(&\underbrace{\sum_{i_1=1}^{N-s+1}\cdots\sum_{i_s=i_{s-1}+1}^{N}}_{s\ \text{sums}}\ \underbrace{\sum_{j_1=1}^{\infty}\cdots\sum_{j_s=1}^{\infty}}_{s\ \text{sums}} C_{i_1\ldots i_s j_1\ldots j_s}^2 \Bigg)
\end{aligned}
\tag{28}
$$

and the PCE error

$$
e_p = \sum_{s=1}^{N}\Bigg(\underbrace{\sum_{i_1=1}^{N-s+1}\cdots\sum_{i_s=i_{s-1}+1}^{N}}_{s\ \text{sums}}\ \underbrace{\sum_{j_1=1}^{\infty}\cdots\sum_{j_s=1}^{\infty}}_{s\ \text{sums};\,j_1+\ldots+j_s>p} C_{i_1\ldots i_s j_1\ldots j_s}^2 \Bigg),
\tag{29}
$$

both consisting of the eliminated PDD coefficients as a result of truncations. In Eq. (28), the first term of the PDD error is due to the truncations of polynomial expansion orders involving main and cooperative effects of at most S variables, whereas the second term of the PDD error is contributed by ignoring the cooperative effects of larger than S variables. In contrast, the PCE error in Eq. (29) derives from the truncations of polynomial expansion orders involving all main and cooperative effects. By selecting $1 \le S \le N$, $1 \le m < \infty$, and $1 \le p < \infty$, the errors can be determined for any PDD and PCE approximations, provided that all coefficients required by Eqs. (28) and (29) can be calculated.

For a general REP, comparing the PDD and PCE errors theoretically based on Eqs. (28) and (29) is not simple, because it depends on which expansion coefficients decay and how they decay with respect to the truncation parameters S, m, and p. However, for a class of problems where the cooperative effects of S input variables on an eigenvalue get progressively weaker as $S \to N$, then the PDD and PCE errors for identical expansion orders can be weighed against each other. For this special case, $m = p$, assume that $C_{i_1\ldots i_s j_1\ldots j_s} = 0$, where $s = S+1,\ldots,N$, $1 \le i_1 < \ldots < i_s \le N$, $j_1,\ldots,j_s = 1,\ldots,\infty$, for both the PDD and PCE approximations. Then, the second term on the right side of Eq. (28) vanishes, resulting in the PDD error

$$
\begin{aligned}
e_{S,m} &= \sum_{s=1}^{S}\Bigg(\underbrace{\sum_{i_1=1}^{N-s+1}\cdots\sum_{i_s=i_{s-1}+1}^{N}}_{s\ \text{sums}}\ \underbrace{\sum_{j_1=m+1}^{\infty}\cdots\sum_{j_s=m+1}^{\infty}}_{s\ \text{sums}} C_{i_1\ldots i_s j_1\ldots j_s}^2 \Bigg) \\
&= \sum_{s=1}^{S}\Bigg(\underbrace{\sum_{i_1=1}^{N-s+1}\cdots\sum_{i_s=i_{s-1}+1}^{N}}_{s\ \text{sums}}\ \underbrace{\sum_{j_1=1}^{\infty}\cdots\sum_{j_s=1}^{\infty}}_{s\ \text{sums}} C_{i_1\ldots i_s j_1\ldots j_s}^2 \Bigg) \\
&\quad - \sum_{s=1}^{S}\Bigg(\underbrace{\sum_{i_1=1}^{N-s+1}\cdots\sum_{i_s=i_{s-1}+1}^{N}}_{s\ \text{sums}}\ \underbrace{\sum_{j_1=1}^{m}\cdots\sum_{j_s=1}^{m}}_{s\ \text{sums}} C_{i_1\ldots i_s j_1\ldots j_s}^2 \Bigg),
\end{aligned}
\tag{30}
$$

while the PCE error can be split into

$$
\begin{aligned}
e_m = & \sum_{s=1}^{S}\left(\underbrace{\sum_{i_1=1}^{N-s+1}\cdots\sum_{i_s=i_{s-1}+1}^{N}}_{s\text{ sums}} \underbrace{\sum_{j_1=1}^{\infty}\cdots\sum_{j_s=1}^{\infty}}_{s\text{ sums}} C_{i_1\ldots i_s j_1\ldots j_s}^2 \right) \\
& - \sum_{s=1}^{S}\left(\underbrace{\sum_{i_1=1}^{N-s+1}\cdots\sum_{i_s=i_{s-1}+1}^{N}}_{s\text{ sums}} \underbrace{\sum_{j_1=1}^{m-s+1}\cdots\sum_{j_s=1}^{m-s+1}}_{s\text{ sums};\, j_1+\ldots+j_s\leq m} C_{i_1\ldots i_s j_1\ldots j_s}^2 \right) \\
\geq & \sum_{s=1}^{S}\left(\underbrace{\sum_{i_1=1}^{N-s+1}\cdots\sum_{i_s=i_{s-1}+1}^{N}}_{s\text{ sums}} \underbrace{\sum_{j_1=1}^{\infty}\cdots\sum_{j_s=1}^{\infty}}_{s\text{ sums}} C_{i_1\ldots i_s j_1\ldots j_s}^2 \right) \\
& - \sum_{s=1}^{S}\left(\underbrace{\sum_{i_1=1}^{N-s+1}\cdots\sum_{i_s=i_{s-1}+1}^{N}}_{s\text{ sums}} \underbrace{\sum_{j_1=1}^{m}\cdots\sum_{j_s=1}^{m}}_{s\text{ sums}} C_{i_1\ldots i_s j_1\ldots j_s}^2 \right) = e_{S,m},
\end{aligned}
\tag{31}
$$

demonstrating larger error from the PCE approximation than from the PDD approximation. In the limit, when $S = N$, similar derivations show $e_m \geq e_{N,m}$, regardless of the values of the expansions coefficients. In other words, the N-variate, mth-order PDD approximation cannot be worse than the mth-order PCE approximation. When $S < N$ and $C_{i_1\ldots i_s j_1\ldots j_s}$, $s = S+1,\ldots,N$, $1 \leq i_1 < \ldots < i_s \leq N$, $j_1,\ldots,j_s = 1,\ldots,\infty$, are not negligible and arbitrary, numerical convergence analysis is required for comparing these two errors.

Remark 6. The stochastic and error analyses aimed at higher-order moments or probability distribution of λ can be envisioned, but no closed-form solutions or simple expressions are possible. However, if λ is sufficiently smooth with respect to $\boldsymbol{X}$—a condition fulfilled by many realistic eigenvalue problems—then Monte Carlo simulation of both the PDD and PCE approximations can be efficiently conducted for also estimating the tail probabilistic characteristics of eigensolutions.

5. CALCULATION OF EXPANSION COEFFICIENTS

The determination of the expansion coefficients required by the PDD or PCE approximation involves various N-dimensional integrals over $\mathbb{R}^N$ and is computationally prohibitive to evaluate when N is arbitrarily large. Instead, a dimension-reduction integration, presented as follows, was applied to estimate the coefficients efficiently [14].

5.1 Dimension-Reduction Integration

Let $\boldsymbol{c} = \{c_1,\ldots,c_N\}^T$ be a reference point of input $\boldsymbol{X}$ and $\lambda(c_1,\ldots,c_{i_1-1},X_{i_1},c_{i_1+1},\ldots,c_{i_{R-k}-1},X_{i_{R-k}},c_{i_{R-k}+1},\ldots,c_N)$ represent an $(R-k)^{\text{th}}$ dimensional component function of $\lambda(\boldsymbol{X})$, where $1 \leq R < N$ is an integer, $k = 0,\ldots,R$, and $1 \leq i_1 < \ldots < i_{R-k} \leq N$. For example, when $R = 1$, the zero-dimensional component function, which is a constant, is $\lambda(\boldsymbol{c})$ and the one-dimensional component functions are $\lambda(X_1,c_2,\ldots,c_N), \lambda(c_1,X_2,\ldots,c_N)$, $\ldots,\lambda(c_1,c_2,\ldots,X_N)$. Using Xu and Rahman's multivariate function theorem [15], it can be shown that the R-variate approximation of $\lambda(\boldsymbol{X})$, defined by

$$
\begin{aligned}
\hat{\lambda}_R(\boldsymbol{X}) := & \sum_{k=0}^{R}(-1)^k \binom{N-R+k-1}{k} \\
& \times \underbrace{\sum_{i_1=1}^{N-R+k+1}\cdots\sum_{i_{R-k}=i_{R-k-1}+1}^{N}}_{(R-k)\text{ sums}} y(c_1,\ldots,c_{i_1-1},X_{i_1},c_{i_1+1},\ldots,c_{i_{R-k}-1},X_{i_{R-k}},c_{i_{R-k}+1},\ldots,c_N),
\end{aligned}
\tag{32}
$$

consists of all terms of the Taylor series of $\lambda(\boldsymbol{X})$ that have less than or equal to R variables. The expanded form of Eq. (32), when compared with the Taylor expansion of $\lambda(\boldsymbol{X})$, indicates that the residual error in $\hat{\lambda}_R(\boldsymbol{X})$ includes terms of dimensions $R+1$ and higher. All higher-order R- and lower-variate terms of $\lambda(\boldsymbol{X})$ are included in Eq. (32), which should therefore generally provide a higher-order approximation of a multivariate function than equations derived from first- or second-order Taylor expansions. Therefore, for $R < N$, an N-dimensional integral can be efficiently estimated by at most R-dimensional integrations, if the contributions from terms of dimensions $R+1$ and higher are negligible.

Substituting $\lambda(\boldsymbol{x})$ in Eqs. (6) and (7) by $\hat{\lambda}_R(\boldsymbol{x})$, the coefficients can be estimated from

$$
\lambda_0 \cong \sum_{k=0}^{R} (-1)^k \binom{N-R+k-1}{k} \underbrace{\sum_{i_1=1}^{N-R+k+1} \cdots \sum_{i_{R-k}=i_{R-k-1}+1}^{N}}_{(R-k) \text{ sums}}
$$
$$
\times \int_{\mathbb{R}^{R-k}} \lambda(c_1, \ldots, c_{i_1-1}, x_{i_1}, c_{i_1+1}, \ldots, c_{i_{R-k}-1}, x_{i_{R-k}}, c_{i_{R-k}+1}, \ldots, c_N) \prod_{q=1}^{R-k} f_{k_q}(x_{k_q}) dx_{k_q}
$$

(33)

and

$$
C_{i_1 \ldots i_s j_1 \ldots j_s} \cong \sum_{k=0}^{R} (-1)^k \binom{N-R+k-1}{k} \underbrace{\sum_{i_1=1}^{N-R+k+1} \cdots \sum_{i_{R-k}=i_{R-k-1}+1}^{N}}_{(R-k) \text{ sums}}
$$
$$
\times \int_{\mathbb{R}^{R-k}_s} \lambda(c_1, \ldots, c_{i_1-1}, x_{i_1}, c_{i_1+1}, \ldots, c_{i_{R-k}-1}, x_{i_{R-k}}, c_{i_{R-k}+1}, \ldots, c_N)
$$
$$
\times \prod_{p=1}^{s} \psi_{i_p j_p}(x_{i_p}) \prod_{q=1}^{R-k} f_{k_q}(x_{k_q}) dx_{k_q},
$$

(34)

which require evaluating at most R-dimensional integrals. Equations (33) and (34), which facilitate calculation of coefficients approaching their exact values as $R \to N$, are more efficient than performing one N-dimensional integration, as in Eqs. (6) and (7), particularly when $R \ll N$. Hence, the computational effort in calculating the coefficients is significantly lowered using the dimension-reduction integration. When $R = 1$, 2, or 3, Eqs. (33) and (34) involve one-, at most two-, and at most three-dimensional integrations, respectively. Nonetheless, numerical integration is still required for a general function λ. The integration points and associated weights depend on the probability distribution of X_i. They are readily available as Gauss-Hermite, Gauss-Legendre, and Gauss-Jacobi quadrature rules when a random variable follows Gaussian, uniform, and β distributions, respectively [8]. In performing the dimension-reduction integration, the value of R should be selected in such a way that it is either equal to or greater than the value of s. Then the expansion coefficient $C_{i_1 \ldots i_s j_1 \ldots j_s}$ will have a nontrivial solution [14].

5.2 Computational Efforts

The S-variate, mth-order PDD approximation requires evaluations of $Q_{S,m} = \sum_{k=0}^{k=S} \binom{N}{S-k} m^{S-k}$ number of PDD coefficients: λ_0 and $C_{i_1 \ldots i_s j_1 \ldots j_s}$, $s = 1, ..., S$, $1 \le i_1 < ... < i_s \le N$, $j_1, ..., j_s = 1, ..., m$. If these coefficients are estimated by dimension-reduction integration with $R = S < N$ and therefore involve, at most, S-dimensional tensor product of an n-point univariate quadrature rule depending on m in Eqs. (33) and (34), then the following deterministic responses (eigenvalue or function evaluations) are required: $\lambda(\boldsymbol{c})$, $\lambda(c_1, ..., c_{i_1-1}, x_{i_1}^{(k_1)}, c_{i_1+1}, ..., c_{i_s-1}, x_{i_s}^{(k_s)}, c_{i_s+1}, ..., c_N)$ for $k_1, ..., k_s = 1, ..., n(m)$, where the superscripts on variables indicate corresponding integration points. Therefore, the total cost for the S-variate, mth-order PDD approximation entails a maximum of $\sum_{k=0}^{k=S} \binom{N}{S-k} n^{S-k}(m)$ eigenvalue evaluations. If the integration points include a common point in each coordinate—a special case of symmetric input probability density functions and odd values of n (see examples 2–5)—the number of eigenvalue evaluations reduces to $\sum_{k=0}^{k=S} \binom{N}{S-k} [n(m)-1]^{S-k}$. In other words, the computational complexity of the PDD approximation is Sth-order polynomial with respect to the number of random variables or integration points.

In contrast, the pth-order PCE approximation requires evaluations of $Q_p = \sum_{k=0}^{N} \binom{N}{N-k} \binom{p}{N-k}$ number of PDD coefficients λ_0 and $C_{i_1 \dots i_s j_1 \dots j_s}$, $s = 1, \dots, N$, $1 \le i_1 < \dots < i_s \le N$, $j_1 + \dots + j_s \le p$, which can again be estimated by dimension-reduction integration by selecting $R = p < N$, and therefore involving, at most, p-dimensional tensor product of an n-point univariate quadrature rule, where n depends on p. As a result, the total cost for the pth-order PCE approximation consists of a maximum of $\sum_{k=0}^{k=p} \binom{N}{p-k} n^{p-k}(p)$ eigenvalue evaluations in general, or $\sum_{k=0}^{k=p} \binom{N}{p-k} [n(p) - 1]^{p-k}$ eigenvalue evaluations for a particular case discussed earlier. In either case, the computational complexity of the PCE approximation is pth-order polynomial with respect to the number of random variables or integration points.

Figures 1a and 1b present plots of the ratio of numbers of eigenvalue evaluations by the PCE and PDD approximations, $\sum_{k=0}^{k=p} \binom{N}{p-k} n^{p-k}(p) / \sum_{k=0}^{k=S} \binom{N}{S-k} n^{S-k}(m)$, as a function of the dimension N for two cases of identical expansion orders $m = p = 3$ and $m = p = 5$, respectively, where $n = m + 1 = p + 1$. The plots in each figure were developed separately for $S = 1$ (univariate), $S = 2$ (bivariate), and $S = 3$ (trivariate) PDD approximations. From the results of Figs. 1a and 1b, regardless of the plot, the ratios are mostly larger than one, indicating greater computational need by the PCE approximation than by the PDD approximation. When $S \ll N$ and $m = p \gg 1$, the PCE approximation is expected to be significantly more expensive than the PDD approximation.

Remark 7. When $S = N$ in PDD or $p \ge N$ in PCE, Eqs. (32)–(34) are irrelevant, eliminating the possibility of any dimension reduction. However, these special cases, evoking merely academic interest, are rarely observed for practical applications with moderate to large numbers of random variables. Nonetheless, the expansion coefficients for these cases can be calculated using the full N-dimensional tensor product of the univariate quadrature formulae, consequently demanding n^N eigenvalue evaluations, where n depends on m or p, for both the PDD and PCE approximations.

6. NUMERICAL EXAMPLES

Five numerical examples involving two well-known mathematical functions and three eigenvalue problems are presented to illustrate the performance of the PDD and PCE approximations for calculating the statistical moments of output functions or eigenvalues, including tail probability distributions of natural frequencies. In examples 1 and 2, the classical Legendre polynomials and associated Gauss-Legendre quadrature formulas were employed to evaluate the expansion coefficients. However, in examples 3–5, all original random variables were transformed into standard Gaussian random variables, employing Hermite orthonormal polynomials as bases and the Gauss-Hermite quadra-
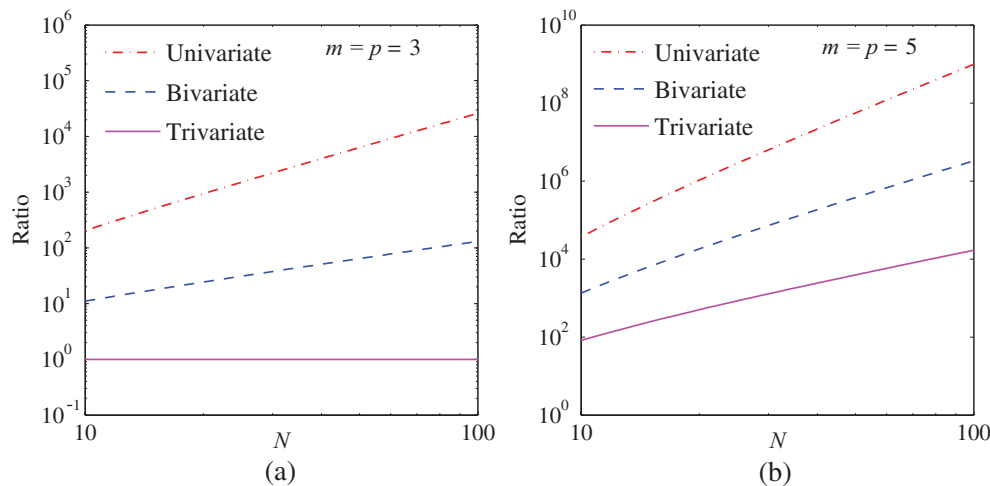

FIG. 1: Ratio of eigenvalue evaluations by the PCE and PDD approximations for two identical polynomial expansion orders: (a) $m = p = 3$ and (b) $m = p = 5$. A ratio greater than one indicates higher computational cost of the PCE approximation than the PDD approximation.

ture rule for calculating the expansion coefficients. The expansion coefficients in example 1 were calculated by full N-dimensional integrations. However, in examples 2–5, the coefficients were estimated by dimension-reduction integration when $S = p < N$, so that an S-variate, mth-order PDD or pth-order PCE approximation requires at most S- or p-dimensional numerical integration. For the third and fourth examples, the eigenvalues were calculated by a hybrid double-shifted LR-QR algorithm [16]. A Lanczos algorithm embedded in the commercial code ABAQUS (Version 6.9) [17] was employed for the fifth example. In examples 3 and 4, the sample sizes for crude Monte Carlo simulation and the embedded Monte Carlo simulation of the PDD and PCE methods are both 10^6. The respective sample sizes are $50,000$ and 10^6 in example 5. The expansion orders m and p vary depending on the example, but in all cases the number of integration points $n = m + 1$ or $n = p + 1$.

6.1 Example 1: Polynomial Function

Consider the polynomial function

$$\lambda(\boldsymbol{X}) = \frac{1}{2^N} \prod_{i=1}^{N} (3X_i^2 + 1) \tag{35}$$

studied by Sudret [18], where X_i, $i = 1, \ldots, N$ are independent and identical random variables, each following standard uniform distribution over [0,1]. From elementary calculations, the exact mean $\mathbb{E}[\lambda(\boldsymbol{X})] = 1$ and the exact variance $\sigma^2 = (6/5)^N - 1$.

The second-moment analysis in this example was conducted for two problem sizes (dimensions): (i) $N = 3$ and (ii) $N = 5$. For $N = 3$, Eq. (35) represents a sixth-order, trivariate, polynomial function, which is a product of three quadratic polynomials in each variable. Therefore, a trivariate, second-order PDD approximation ($S = 3$, $m = 2$) with second-order Legendre polynomials (interval $= [-1, +1]$) in Eq. (15) should exactly reproduce λ. Since X_1, X_2, and X_3 are independent, the highest order of integrands for calculating the expansion coefficients is 4. A three-point Gauss-Legendre quadrature should then provide the exact values of all coefficients. Therefore, if the expansion coefficients are calculated using $m \geq 2$ in Eq. (15), and Eqs. (6) and (7) are numerically integrated with $n \geq m + 1$, then the only source of error in a truncated PDD is the selection of S.

For $N = 3$, Table 2 presents the relative errors, defined as the ratio of the absolute difference between the exact and approximate variances of $\lambda(\boldsymbol{X})$ to the exact variance of $\lambda(\boldsymbol{X})$, from the univariate ($S = 1$), bivariate ($S = 2$), and trivariate ($S = 3$) PDD approximations. They were calculated for m varying from one to six, involving eight to 343

TABLE 2: Relative errors in calculating the variance of the polynomial function for $N = 3$ by the PDD and PCE approximations (example 1)

m or p	PDD[a] $S = 1$	$S = 2$	$S = 3$	PCE[a]	No. of function evaluations[b]
1	2.273×10^{-1}	8.246×10^{-2}	7.341×10^{-2}	2.273×10^{-1}	8
2	1.758×10^{-1}	1.099×10^{-2}	0	3.095×10^{-2}	27
3	1.758×10^{-1}	1.099×10^{-2}	$-$[c]	2.578×10^{-3}	64
4	1.758×10^{-1}	1.099×10^{-2}	$-$[c]	1.234×10^{-4}	125
5	1.758×10^{-1}	1.099×10^{-2}	$-$[c]	2.683×10^{-6}	216
6	1.758×10^{-1}	1.099×10^{-2}	$-$[c]	0	343

[a] The variances from trivariate PDD for $m = 2$ and PCE for $p = 6$ coincide with the exact solution: $\sigma^2 = (6/5)^N - 1$, where $N = 3$.

[b] The number of function evaluations by all three PDD and PCE methods employing a full N-dimensional numerical integration and n-point univariate Gauss-Legendre rule is n^N, where $N = 3$, $n = m + 1$, and $1 \leq m \leq 6$.

[c] Not required.

function evaluations, respectively, when estimating the expansion coefficients by full N-dimensional integrations. The errors from all three PDD approximations drop as m increases, but they level off quickly at their respective limits for the univariate and bivariate PDD approximations. When $m = 2$, the error due to the trivariate PDD approximation is zero as the PDD approximation coincides with $\lambda(\boldsymbol{X})$ in Eq. (35), as expected. For comparison, the same problem was solved using the PCE approximation with p varying from 1 to 6 and correspondingly requiring eight to 343 function evaluations. The relative errors by the PCE approximation enumerated in Table 2 also converge to zero, but at an expansion order $p = 6$, which is three times larger than the order of univariate polynomials required by the PDD method. At exactness, the PDD method is more efficient than the PCE method by a factor of $343/27 \cong 13$.

The function in Eq. (35) was also studied for a slightly larger dimension: $N = 5$. The associated errors of the pentavariate ($S = 5$) PDD approximation and PCE approximation with several polynomial expansion orders are displayed in Table 3. Again, both the PDD and PCE methods produce zero errors, however, at the cost of second- and 10th-order expansions, respectively. As a result, the factor of efficiency of the PDD method jumps to $161051/243 \cong 663$, even for such a small increase in the dimension. The higher efficiency of the PDD approximation for both problem sizes is attributed to its dimensional hierarchy, favorably exploiting the structure of λ.

6.2 Example 2: Non-Polynomial Function

The second example involves second-moment analysis of the Ishigami and Homma function [19]

$$\lambda(\boldsymbol{X}) = \sin X_1 + a \sin^2 X_2 + b X_3^4 \sin X_1, \tag{36}$$

where X_i, $i = 1, 2, 3$, are three independent and identically distributed uniform random variables on $[-\pi, +\pi]$, and a and b are real-valued deterministic parameters. This function also permits the exact solution of the variance: $\sigma^2 = a^2/8 + b\pi^4/5 + b^2\pi^8/18 + 1/2$. Note that λ is a nonpolynomial function; therefore, neither the PDD nor the PCE approximation will provide the exact solution, but their respective errors can be reduced to an arbitrarily low value

TABLE 3: Relative errors in calculating the variance of the polynomial function for $N = 5$ by the PDD and PCE approximations (example 1)

m or p	Pentavariate PDD $(S = 5)$[a]	PCE[a]	No. of function evaluations[b]
1	8.528×10^{-1}	3.700×10^{-1}	32
2	0	9.189×10^{-2}	243
3	—[c]	1.610×10^{-2}	1024
4	—[c]	2.042×10^{-3}	3125
5	—[c]	1.882×10^{-4}	7776
6	—[c]	1.240×10^{-5}	16,807
7	—[c]	5.590×10^{-7}	32,768
8	—[c]	1.558×10^{-8}	59,049
9	—[c]	2.050×10^{-10}	100,000
10	—[c]	0	161,051

[a] The variances from trivariate PDD for $m = 2$ and PCE for $p = 10$ coincide with the exact solution: $\sigma^2 = (6/5)^N - 1$, where $N = 5$.

[b] The number of function evaluations by the PDD and PCE methods employing a full N-dimensional numerical integration and n-point univariate Gauss-Legendre rule is n^N, where $N = 5$, $n = m + 1$, and $1 \le m \le 10$.

[c] Not required.

by increasing the polynomial expansion orders successively. In this example, the following deterministic parameters were selected: $a = 7$, $b = 0.1$.

Since the right hand side of Eq. (36) includes the cooperative effects of at most two variables, the bivariate PDD approximation is adequate for convergence analysis. In this example, the PDD expansion coefficients of the bivariate approximation were estimated using Legendre polynomials (interval $= [-1, +1]$) of a specified order m and dimension-reduction integration (Gauss-Legendre quadrature rule) with $R = S = 2$, and $n = m + 1$. Several even orders, $m = 2, 4, 6, 8, 10, 12, 14, 16, 18$, were chosen in such a way that n remained an odd integer. In so doing, the corresponding number of function evaluations by the PDD method for a given m is $3m^2 + 3m + 1$. For the PCE approximation, the PDD expansion coefficients for a specified order $2 \le p \le 18$ and $n = p + 1$ were calculated by dimension-reduction integration when $p < 3$ involving $\sum_{k=0}^{k=p} \binom{3}{p-k}(n-1)^{p-k}$ function evaluations for even p and full three-dimensional integration when $p \ge 3$ involving n^3 function evaluations.

Figure 2 shows how the relative errors in the variances of $\lambda(\boldsymbol{X})$ from the bivariate PDD and PCE approximations vary with respect to the number (L) of function evaluations. The data points of these plots were generated by calculating the approximate variances for the selected values of m or p and counting the corresponding number of functions evaluations. Ignoring the first three data points in Fig. 2, the errors of the PDD and PCE solutions decay proportionally to $L^{-17.5}$ and $L^{-12.1}$, respectively. Clearly, their convergence rates—the absolute values of the slopes of the trend lines in the log-log plots—are much higher than unity. The sampling-based methods, crude Monte Carlo, and quasi-Monte Carlo, which have theoretical convergence rates in the range of 0.5–1 are no match for the PDD and PCE methods, which are endowed with significantly higher convergence rates, mostly due to the smoothness of λ. Furthermore, the PDD approximation converges markedly faster than the PCE approximation. Although a similar observation was made in example 1, the validity of this trend depends on the function examined.

6.3 Example 3: Two-Degree-of-Freedom, Undamped, Spring-Mass System

Consider a two-degree-of-freedom, undamped, spring-mass system, shown in Fig. 3, with random or deterministic mass and random stiffness matrices

$$\boldsymbol{M} = \begin{bmatrix} M_1(\boldsymbol{X}) & 0 \\ 0 & M_2(\boldsymbol{X}) \end{bmatrix} \text{ and } \boldsymbol{K}(\boldsymbol{X}) = \begin{bmatrix} K_1(\boldsymbol{X}) + K_3(\boldsymbol{X}) & -K_3(\boldsymbol{X}) \\ -K_3(\boldsymbol{X}) & K_2(\boldsymbol{X}) + K_3(\boldsymbol{X}) \end{bmatrix}, \tag{37}$$
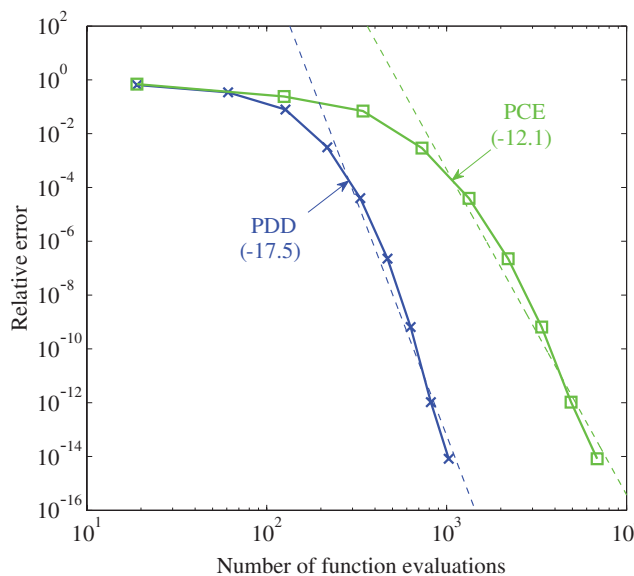
FIG. 2: Relative errors in calculating the variance of the Ishigami and Homma [19] function by the PDD and PCE approximations (example 2). The parenthetical values denote slopes of the trend lines
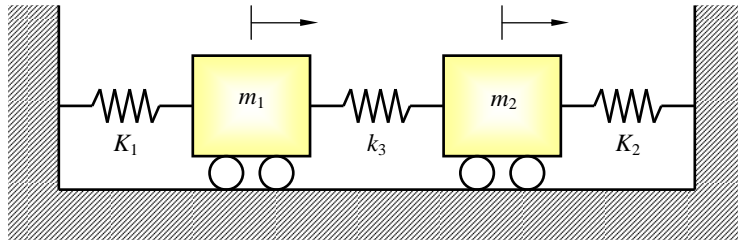
FIG. 3: Two-degree-of-freedom, undamped, spring-mass system

respectively, where $K_1(\boldsymbol{X}) = 1000X_1$ N/m, $K_2(\boldsymbol{X}) = 1100X_2$ N/m, $K_3(\boldsymbol{X}) = 100X_3$ N/m, $M_1(\boldsymbol{X}) = X_4$ kg, and $M_2(\boldsymbol{X}) = 1.5X_5$ kg. The input $\boldsymbol{X} = \{X_1, X_2, X_3, X_4, X_5\}^T \in \mathbb{R}^5$ is an independent lognormal random vector with the mean vector $\boldsymbol{\mu_X} = \mathbf{1} \in \mathbb{R}^5$ and covariance matrix $\boldsymbol{\Sigma_X} = \mathrm{diag}(v_1^2, v_2^2, v_3^2, v_4^2, v_5^2) \in \mathbb{R}^{5\times5}$, where v_i represents the coefficient of variation of X_i. Two cases of the problem size based on the coefficients of variations were examined: (i) $N = 2$ with $v_1 = v_2 = 0.25$, $v_3 = v_4 = v_5 = 0$; and (ii) $N = 5$ with $v_1 = v_2 = 0.25$, $v_3 = v_4 = v_5 = 0.125$. The first case comprises uncertain stiffness properties of the first two springs only, whereas the second case includes uncertainties in all mass and stiffness properties. In both cases, there exist two real-valued random eigenvalues, $\lambda_1(\boldsymbol{X})$ and $\lambda_2(\boldsymbol{X})$, which are sorted into an ascending order.

Since the eigenvalues are in general non-polynomial functions of input, a convergence study with respect to the truncation parameters of PDD and PCE is required to calculate the probabilistic characteristics of eigensolutions accurately. Figures 4a and 4b depict how the normalized errors of the second-moment properties, $e_{S,m}/\mathbb{E}\left[\lambda(\boldsymbol{X}) - \lambda_0\right]^2$
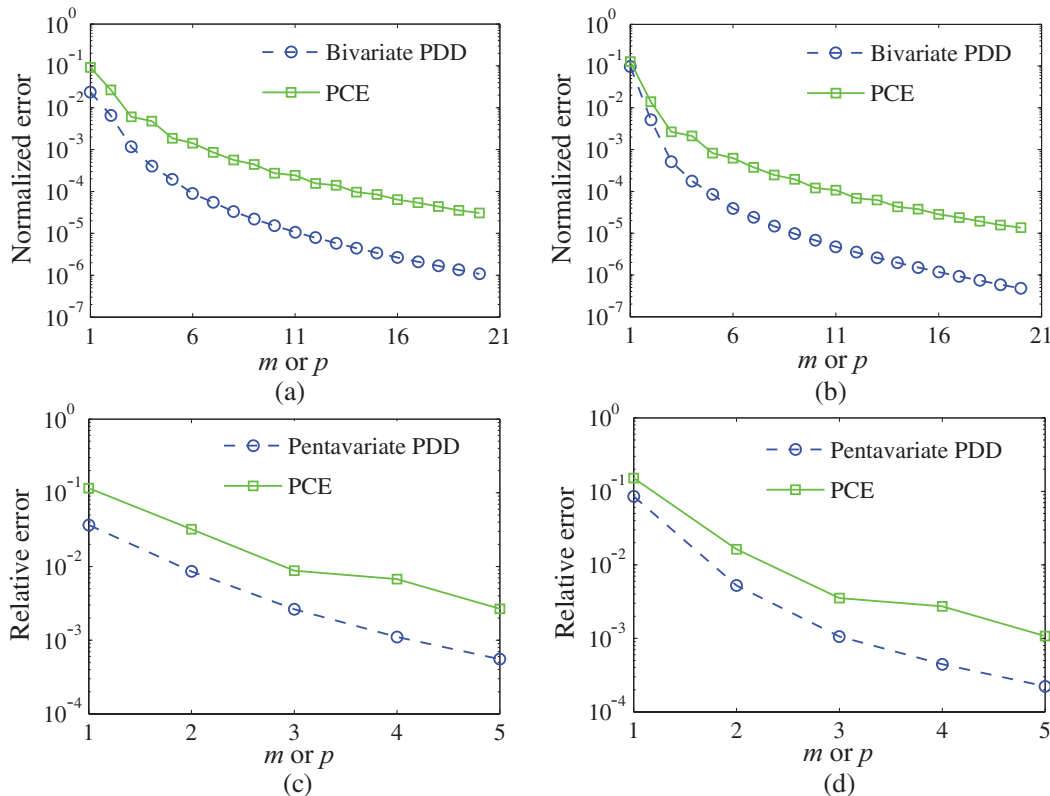

FIG. 4: Errors in calculating the variances of eigenvalues of the two-degree-of-freedom oscillator by the PDD and PCE approximations (example 3): (a) first eigenvalue ($N = 2$), (b) second eigenvalue ($N = 2$), (c) first eigenvalue ($N = 5$), and (d) second eigenvalue ($N = 5$)

and $e_p/\mathbb{E}\left[\lambda(\boldsymbol{X}) - \lambda_0\right]^2$, of the the first and second eigenvalues, respectively, decay with respect to m or p for $N = 2$. The normalized errors were calculated using Eqs. (20), (28), and (29) and employing the value of 80, a sufficiently large integer, for replacing the infinite limits of the summations. For any identical expansion orders ($m = p$), the bivariate PDD approximation ($S = N = 2$) yields smaller errors than the PCE approximation, consistent with the theoretical finding described in Section 4.3. As soon as m or p becomes >3, the difference in the errors by the PDD and PCE approximations grows by more than an order of magnitude.

For a case of larger dimension ($N = 5$), calculating the normalized errors in the same way as described above requires an enormous number of PDD coefficients. In addition, the determination of these coefficients is computationally taxing, if not prohibitive, considering infinite limits in Eqs. (20), (28), and (29). To circumvent this problem, another relative error, defined as the ratio of the absolute difference between the numerically integrated and approximate variances of $\lambda(\boldsymbol{X})$ to the numerically integrated variance of $\lambda(\boldsymbol{X})$, employing the pentavariate ($S = 5$) PDD [Eq. (19)] or PCE [Eq. (25)] approximation, was evaluated. The variance estimated by numerical integration involved a full five-dimensional tensor product of a 25-point univariate quadrature rule, where the number of integration points was ascertained adaptively. The plots of the relative error versus m or p in Fig. 4c and 4d for first and second eigenvalues, respectively, display a trend similar to that observed when $N = 2$, verifying once again that the errors from the PDD approximation are always smaller than those from the PCE approximation. In other words, the PDD method is expected to predict more accurate second-moment properties of random eigensolutions than the PCE method for, at least, the simple dynamic systems examined in this work.

6.4 Example 4: Free-Standing Beam

The fourth example involves free vibration of a tall, free-standing beam shown in Fig. 5a [20]. Figure 5b represents a lumped-parameter model of the beam, which comprises seven rigid, massless links hinged together. The mass of
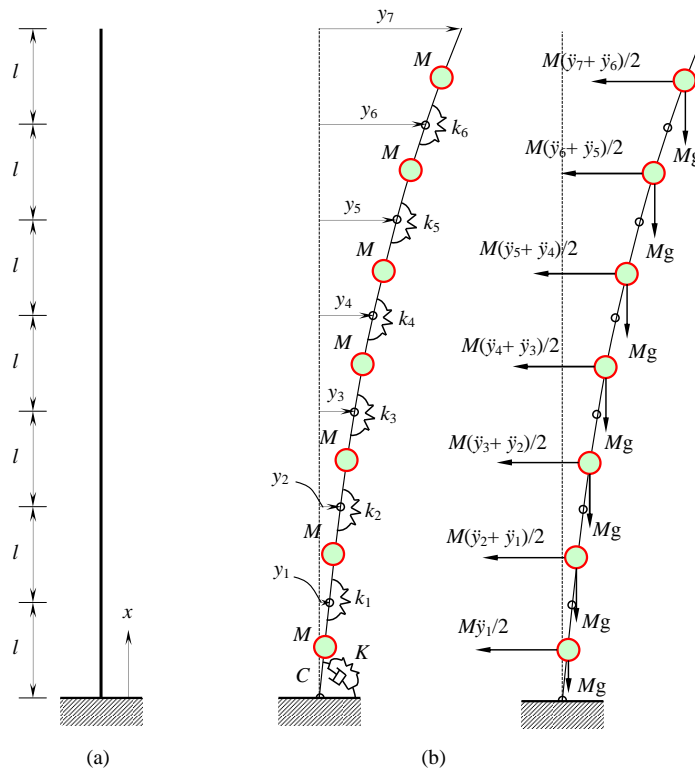

FIG. 5: Free-standing beam: (a) continuous representation and (b) seven-degree-of-freedom discrete model

the beam is represented by seven random point masses located at the center of each link. No damping was assumed, except at the bottom joint, where the random, rotational, viscous damping coefficient due to the foundation pad is C. The random rotational stiffness at the bottom of the beam, controlled by the lower half of the bottom link and the flexibility of the foundation pad, is K. The independent random variables M, C, and K are lognormally distributed with respective means of 3000 kg, 2×10^7 N-m-s/rad, and 2×10^9 N-m/rad and have a 20% coefficient of variation. The flexural rigidity of the beam is represented by six rotational springs between links with stiffnesses $k(x) = k(x_i)$, $i = 1, \ldots, 6$, where $x_i = il$, $i = 1, \ldots, 6$, and $l = 6$ m. The spatially varying spring stiffness $k(x) = c_\alpha \exp[\alpha(x)]$ is an independent, homogeneous, lognormal random field with mean $\mu_k = 2 \times 10^9$ N-m/rad and coefficient of variation $v_k = 0.2$, where $c_\alpha = \mu_k/\sqrt{1 + v_k^2}$ and $\alpha(x)$ is a zero-mean, homogeneous, Gaussian random field with variance $\sigma_\alpha^2 = \ln(1 + v_k^2)$ and covariance function $\Gamma_\alpha(u) := \mathbb{E}[\alpha(x)\alpha(x+u)] = \sigma_\alpha^2 \exp(-|u|/l)$. A discretization of $\alpha(x)$ yields the zero-mean Gaussian random vector $\boldsymbol{\alpha} = \{\alpha_1, \ldots, \alpha_6\}^T := \{\alpha(l), \ldots, \alpha(6l)\}^T \in \mathbb{R}^6$ with covariance matrix $\boldsymbol{\Sigma}_\alpha := [\mathbb{E}(\alpha_u \alpha_v)]$, $u, v = 1, \ldots, 6$, where $\mathbb{E}(\alpha_u \alpha_v) = \mathbb{E}[\alpha(ul)\alpha(vl)] = \Gamma_\alpha[(u - v)l]$, providing complete statistical characterization of spring stiffnesses $k_i = c_\alpha \exp(\alpha_i)$. Therefore, the input random vector $\boldsymbol{X} = \{M, C, K, \alpha_1, \ldots, \alpha_6\}^T \in \mathbb{R}^9$ includes nine random variables in this example. Further details of the dynamic system, including mass, damping, and stiffness matrices, are available in the authors' prior work [20].

Due to nonproportional damping, the discrete beam model yields 14 complex eigenvalues $\lambda_i(\boldsymbol{X}) = \lambda_{R,i}(\boldsymbol{X}) \pm \sqrt{-1}\lambda_{I,i}(\boldsymbol{X})$, $i = 1, \ldots, 7$ in conjugate pairs, where the real parts $\lambda_{R,i}(\boldsymbol{X})$ and imaginary parts $\lambda_{I,i}(\boldsymbol{X})$ are both stochastic. Using the PDD method, Fig. 6 presents the marginal probability distributions $F_{I,i}(\lambda_{I,i})$ and the complementary probabilities $1 - F_{I,i}(\lambda_{I,i})$, $i = 1, \ldots, 7$ of all seven imaginary parts, which also represent the natural frequencies of the beam. The distributions $F_{I,i}(\lambda_{I,i})$ and $1 - F_{I,i}(\lambda_{I,i})$ at low probabilities describe tail characteristics of λ_i at the left and right ends, respectively. Each subfigure of Fig. 6 contains four plots: one obtained from crude Monte Carlo simulation and the remaining three generated from the univariate ($S = 1$), bivariate ($S = 2$), and trivariate ($S = 3$) PDD approximations, employing $m = 3$, $n = 4$. In contrast, Fig. 7 displays the same probability distributions of all seven imaginary parts of the eigenvalues calculated using the PCE method. Each subfigure of Fig. 7 also contains four plots: one obtained from crude Monte Carlo simulation and the remaining three derived from the first-order ($p = 1$), second-order ($p = 2$), and third-order ($p = 3$) PCE approximations, employing $n = p + 1$. From Fig. 6 or 7, the tail probability distributions at both ends converge rapidly with respect to S or p, regardless of the oscillatory mode. Therefore, both the PDD and PCE methods can be applied to solve this REP accurately.

To determine the computational efficiency of the PDD and PCE methods, Figs. 8a and 8b portray enlarged views of the tail probability distributions of the first and seventh natural frequencies, respectively, of the beam calculated by all three variants of the PDD or PCE methods, including crude Monte Carlo simulation. Compared with crude Monte Carlo simulation, the bivariate, third-order PDD approximation, trivariate, third-order PDD approximation, and third-order PCE approximation provide excellent estimates of the tail distributions. The results further indicate that the bivariate, third-order PDD and third-order PCE approximations, both in consilience with the Monte Carlo solution, demand 613 and 5989 eigenvalue evaluations. Therefore, the PDD approximation is about $5989/613 \cong 10$ times more economical than the PCE approximation.

6.5 Example 5: Piezoelectric Transducer

The final example entails eigenspectrum analysis of a piezoelectric transducer commonly used for converting electrical pulses to mechanical vibrations, and vice versa. Figure 9a shows a 25 mm diam cylinder made of a piezoelectric ceramic PZT4 (lead zirconate titanate) with brass end caps. The thicknesses of the transducer and end caps are 1.5 and 3 mm, respectively. The cylinder, 25 mm long, was electroded on both the inner and outer surfaces. The random variables include: (i) ten nonzero constants defining elasticity, piezoelectric stress coefficients, and dielectric properties of PZT4; (ii) elastic modulus and Poisson's ratio of brass; and (iii) mass densities of brass and PZT4 [7]. The statistical properties of all 14 random variables are listed in Table 4. The random variables are independent and follow lognormal distributions. Because of axisymmetry, a 20-noded finite-element model of a slice of the transducer, shown in Fig. 9b, was created. The model was considered to be open circuited. All natural frequencies calculated correspond to antiresonant frequencies.
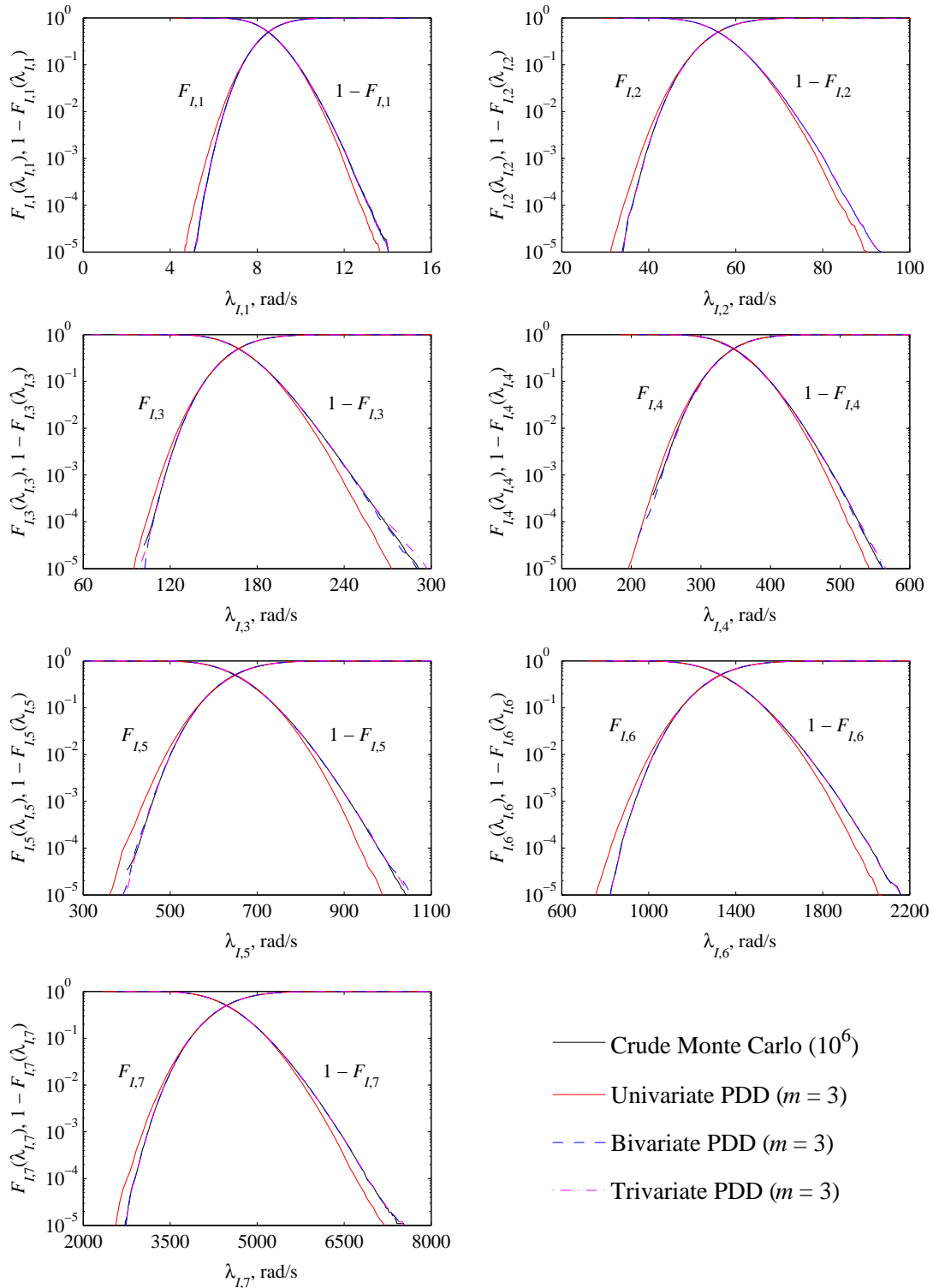
FIG. 6: Tail probability distributions of the imaginary parts of eigenvalues of the free-standing beam by the PDD and crude Monte Carlo methods (example 4)
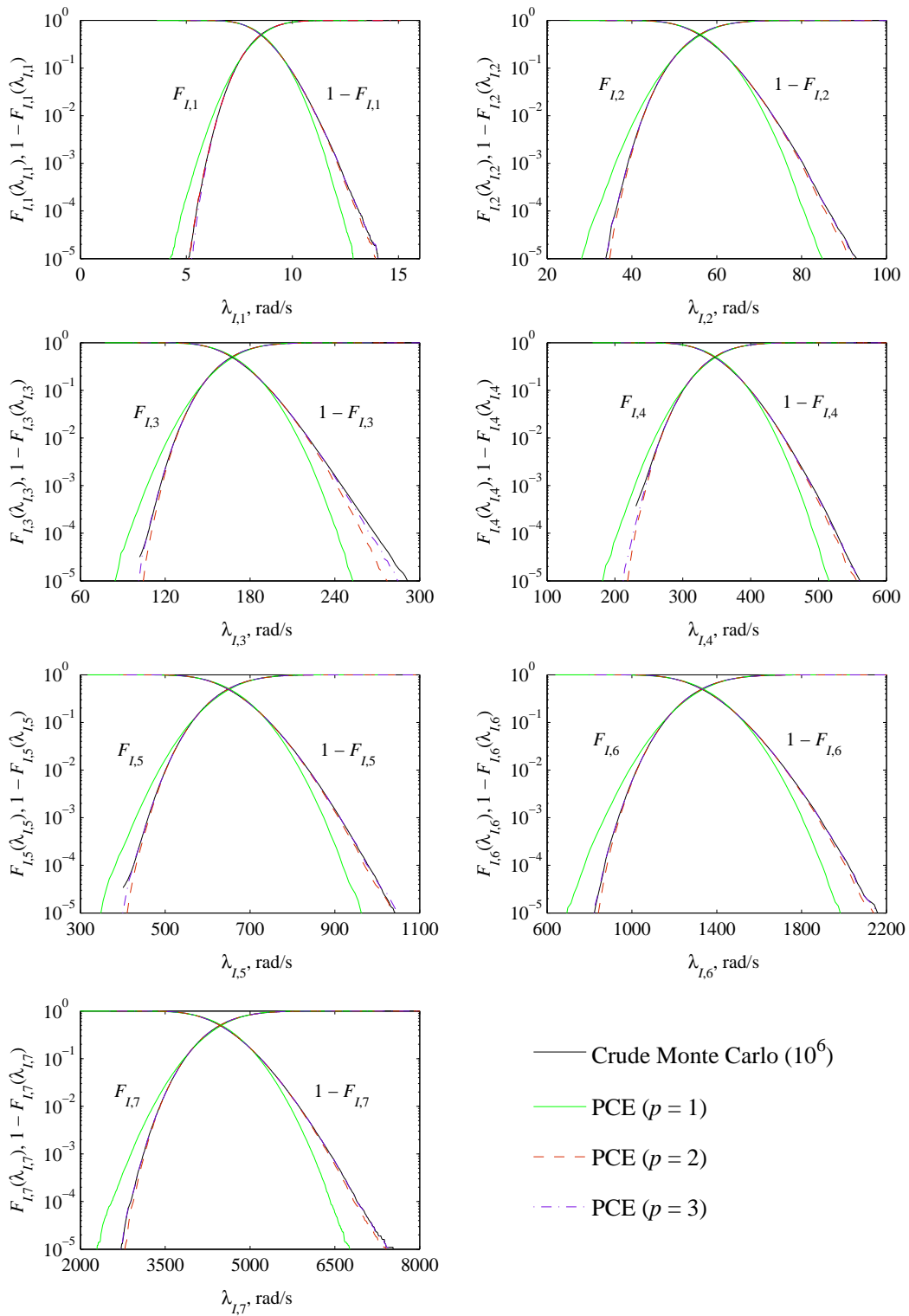
FIG. 7: Tail probability distributions of the imaginary parts of eigenvalues of the free-standing beam by the PCE and crude Monte Carlo methods (example 4)
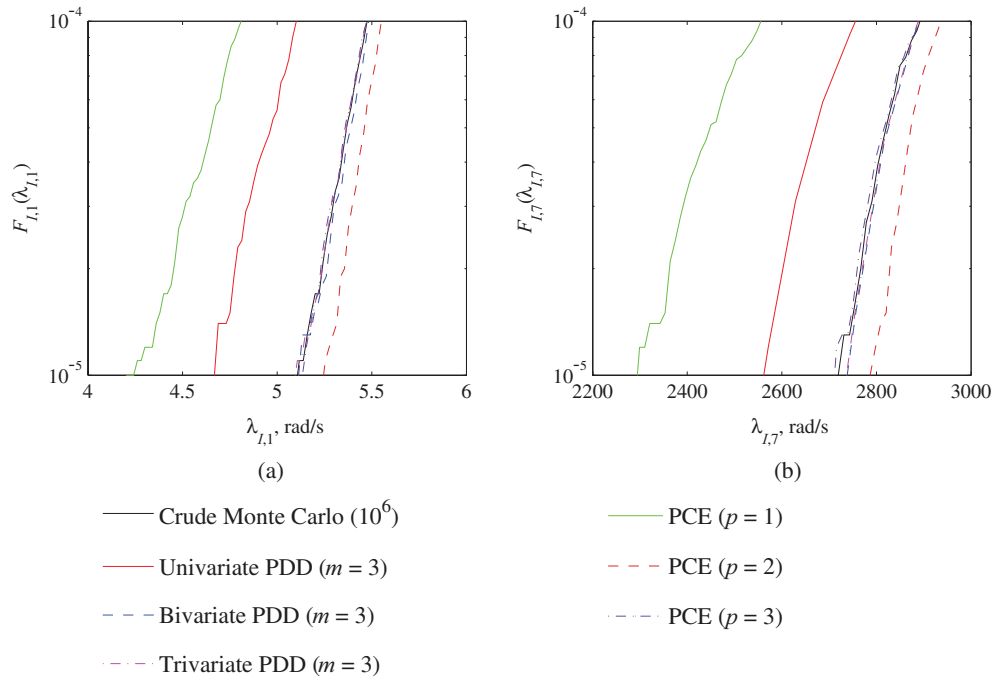
FIG. 8: Comparisons of tail probability distributions of the imaginary parts of eigenvalues of the free-standing beam by the PDD, PCE, and crude Monte Carlo methods (example 4): (a) $\lambda_{I,1}$ and (b) $\lambda_{I,7}$
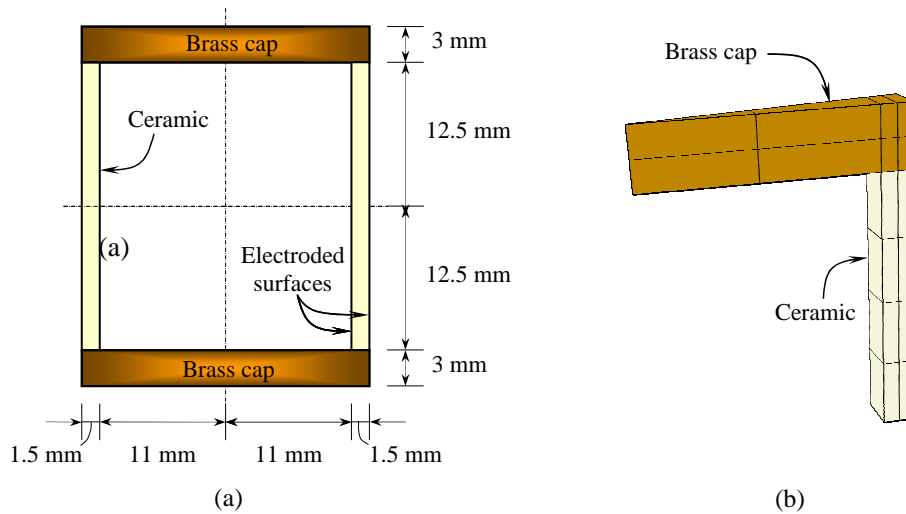

FIG. 9: Piezoelectric transducer: (a) geometry and (b) finite-element discrete model

Figure 10 presents the marginal probability distributions of the first six natural frequencies, Ω_i, $i = 1, \ldots, 6$, of the transducer by the bivariate ($S = 2$), third-order ($m = 3$) PDD and third-order ($p = 3$) PCE methods, respectively. These probabilistic characteristics, obtained by setting $n = m + 1 = p + 1 = 4$, are judged to be converged responses, as their changes due to further increases in m and p are negligibly small. Therefore, the PDD and PCE methods require 1513 and 24,809 ABAQUS-aided FEA, respectively—a significant mismatch in computational efforts—in

TABLE 4: Statistical properties of the random input for the piezoelectric cylinder

Random variable	Property[a]	Mean	Coefficient of variation
X_1, GPa	D_{1111}	115.4	0.15
X_2, GPa	D_{1122}, D_{1133}	74.28	0.15
X_3, GPa	D_{2222}, D_{3333}	139	0.15
X_4, GPa	D_{2233}	77.84	0.15
X_5, GPa	$D_{1212}, D_{2323}, D_{1313}$	25.64	0.15
X_6, Coulomb/m^2	e_{111}	15.08	0.1
X_7, Coulomb/m^2	e_{122}, e_{133}	–5.207	0.1
X_8, Coulomb/m^2	e_{212}, e_{313}	12.71	0.1
X_9, nF/m	D_{11}	5.872	0.1
X_{10}, nF/m	D_{22}, D_{33}	6.752	0.1
X_{11}, GPa	E_b	104	0.15
X_{12}	ν_b	0.37	0.05
X_{13}, g/m^3	ρ_b	8500	0.15
X_{14}, g/m^3	ρ_c	7500	0.15

[a] D_{ijkl} are elastic moduli of ceramic; e_{ijk} are piezoelectric stress coefficients of ceramic; D_{ij} are dielectric constants of ceramic; E_b, ν_b, ρ_b are elastic modulus, Poisson's ratio, and mass density of brass; ρ_c is mass density of ceramic.

generating all six probability distributions. Due to expensive FEA, crude Monte Carlo simulation was conducted only up to 50,000 realizations, producing only rough estimates of the distributions. Given the low sample size, the distributions from crude Monte Carlo simulation, also plotted in Fig. 10, are not expected to provide very accurate tail characteristics. Nonetheless, the overall shapes of all six probability distributions generated by both expansion methods match these Monte Carlo results quite well. However, a comparison of their computational efforts once again finds the PDD method wringing computational savings more than the PCE method by an order of magnitude in solving this practical eigenvalue problem.

7. CONCLUSIONS

Two stochastic expansion methods originating from PDD and PCE were investigated for solving REPs commonly encountered in stochastic dynamic systems. Both methods comprise a broad range of orthonormal polynomial bases consistent with the probability measure of the random input and an innovative dimension-reduction integration for calculating the expansion coefficients. A new theorem, proven herein, demonstrates that the infinite series from PCE can be reshuffled to derive the infinite series from PDD and vice versa. However, compared with PCE, which contains terms arranged with respect to the order of polynomials, PDD is structured with respect to the degree of cooperativity between a finite number of random variables. Therefore, significant differences exist regarding the accuracy, efficiency, and convergence properties of their truncated series.

An alternative form of the PCE approximation expressed in terms of the PDD expansion coefficients was developed. As a result, the probabilistic eigensolutions from both the PDD and PCE methods can be obtained from the same PDD coefficients, leading to closed-form expressions of the second-moment properties of eigenvalues and respective errors. For a class of REPs, where the cooperative effects of input variables on an eigenvalue get progressively weaker or vanish altogether, the error perpetrated by the PCE approximation is larger than that committed by the PDD approximation, when the expansions orders are equal. Given the same expansion orders, the PDD approximation in-
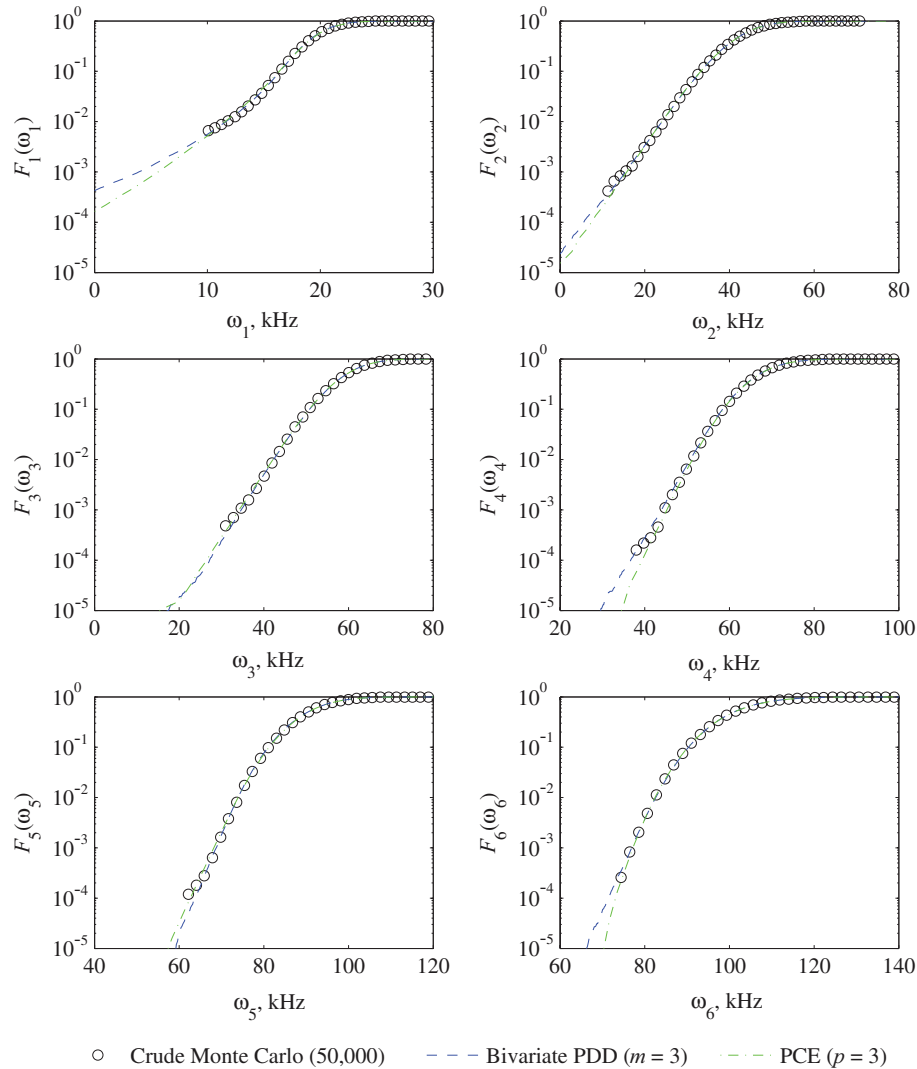
FIG. 10: Marginal probability distributions of the first six natural frequencies of the piezoelectric transducer by the PDD, PCE, and crude Monte Carlo methods (example 5)

cluding main and cooperative effects of all input variables cannot be worse than the PCE approximation, although the inclusion of all cooperative effects undermines the salient features of PDD.

The PDD and PCE methods were employed to calculate the second-moment properties and tail probability distributions in five numerical problems, where the output functions are either mathematical functions involving smooth polynomials or nonpolynomials or real- or complex-valued eigensolutions from dynamic systems, some requiring FEA. The second-moment errors from the mathematical functions indicate rapid convergence of the PDD and PCE solutions, easily outperforming the sampling-based methods. Moreover, for the functions examined, the convergence rates of the PDD method are noticeably higher than those of the PCE approximation. The same trend was observed when calculating the variance of a two-degree-of-freedom linear oscillator regardless of the number of random variables. A comparison of the numbers of eigenvalue evaluations (numbers of FEA), required for estimating with the same accuracy the frequency distributions of a free-standing beam and a piezoelectric transducer, finds the PDD approximation to be more economical than the PCE approximation by an order of magnitude or more. The computational

efficiency of the PDD method is attributed to its dimensional hierarchy, favorably exploiting the hidden dimensional structures of stochastic responses, including random eigensolutions, examined in this work.

ACKNOWLEDGMENTS

REFERENCES

1. Boyce, W. E., *Probabilistic Methods in Applied Mathematics I*, Academic Press, New York, 1968.

2. Mehlhose, S., Vom Scheidt, J., and Wunderlich, R., Random eigenvalue problems for bending vibrations of beams, *Zeit. Angew. Math. Mech.*, 79:693–702, 1999.

3. Grigoriu, M., A solution of the random eigenvalue problem by crossing theory, *J. Sound Vib.*, 158(1):69–80, 1992.

4. Nair, P. B. and Keane, A. J., An approximate solution scheme for the algebraic random eigenvalue problem, *J. Sound Vib.*, 260(1):45–65, 2003.

5. Adhikari, S. and Friswell, M. I., Random matrix eigenvalue problems in structural dynamics, *Int. J. Numer. Methods Eng.*, 69:562–591, 2007.

6. Ghosh, D., Ghanem, R. G., and Red-Horse, J., Analysis of eigenvalues and modal interaction of stochastic systems, *AIAA Jo.*, 43:2196–2201, 2005.

7. Rahman, S., Probability distributions of natural frequencies of uncertain dynamic systems, *AIAA J.*, 47(6):1579–1589, 2009.

8. Gautschi, W., *Orthogonal Polynomials: Computation and Approximation*, Oxford University Press, London, 2004.

9. Rahman, S., Extended polynomial dimensional decomposition for arbitrary probability distributions, *J. Eng. Mech.*, 135(12):1439–1451, 2009.

10. Rahman, S., Statistical moments of polynomial dimensional decomposition, *J. Eng. Mech.*, 136(7):923–927, 2010.

11. Wiener, N., The homogeneous chaos, *Am. J. Math.*, 60(4):897–936, 1938.

12. Ghanem, R. G. and Spanos, P. D., *Stochastic Finite Elements: A Spectral Approach*, Springer-Verlag, Berlin, 1991.

13. Xiu, D. and Karniadakis, G. E., The Wiener-Askey polynomial chaos for stochastic differential equations, *SIAM J. Sci. Comput.*, 24:619–644, 2002.

14. Rahman, S., A polynomial dimensional decomposition for stochastic computing, *Int. J. Numer. Methods Eng.*, 76:2091–2116, 2008.

15. Xu, H. and Rahman, S., A generalized dimension-reduction method for multi-dimensional integration in stochastic mechanics, *Int. J. Numer. Methods Eng.*, 61:1992–2019, 2004.

16. IMSL Numerical Libraries, *User's Guide and Theoretical Manual*, Visual Numerics, Houston, Texas, 2005.

17. ABAQUS Standard, Version 6.9, Dassualt Systems Simulia Corp., 2010.

18. Sudret, B., Global sensitivity analysis using polynomial chaos expansions, *Reliab. Eng. Sys. Safety*, 93(7):964–979, 2008.

19. Ishigami, T. and Homma, T., An importance quantification technique in uncertainty analysis for computer models, *Proceedings of the ISUMA '90, 1st International Symposium on Uncertainty Modeling and Analysis*, University of Maryland, pp. 398–403, 1990.

20. Rahman, S., Stochastic dynamic systems with complex-valued eigensolutions, *Int. J. Numer. Methods Eng.*, 71:963–986, 2007.